

# THE PROPAGATION OF UNCERTAINTIES IN STELLAR POPULATION SYNTHESIS MODELING I: THE RELEVANCE OF UNCERTAIN ASPECTS OF STELLAR EVOLUTION AND THE IMF TO THE DERIVED PHYSICAL PROPERTIES OF GALAXIES

CHARLIE CONROY AND JAMES E. GUNN

Department of Astrophysical Sciences, Princeton University, Princeton, NJ 08544, USA

MARTIN WHITE

Departments of Physics and Astronomy, 601 Campbell Hall, University of California Berkeley, CA 94720, USA

*Submitted to the Astrophysical Journal*

## ABSTRACT

The stellar masses, mean ages, metallicities, and star formation histories of galaxies are now commonly estimated via stellar population synthesis (SPS) techniques. SPS relies on stellar evolution calculations from the main sequence to stellar death, stellar spectral libraries, phenomenological dust models, and stellar initial mass functions (IMFs) to translate the evolution of a multi-metallicity, multi-age set of stars into a prediction for the time-evolution of the integrated light from that set of stars. Each of these necessary inputs carries significant uncertainties that have until now received little systematic attention. The present work is the first in a series that explores the impact of uncertainties in key phases of stellar evolution and the IMF on the derived physical properties of galaxies and the expected luminosity evolution for a passively evolving set of stars. A Monte-Carlo Markov-Chain approach is taken to fit near-UV through near-IR photometry of a representative sample of low- and high-redshift galaxies with this new SPS model. Significant results include the following: 1) including uncertainties in stellar evolution, stellar masses at  $z \sim 0$  carry errors of  $\sim 0.3$  dex at 95% CL with little dependence on luminosity or color, while at  $z \sim 2$ , the masses of bright red galaxies are uncertain at the  $\sim 0.6$  dex level; 2) either current stellar evolution models, current observational stellar libraries, or both, do not adequately characterize the metallicity-dependence of the thermally-pulsating asymptotic giant branch phase; 3) conservative estimates on the uncertainty of the slope of the IMF in the solar neighborhood imply that luminosity evolution per unit redshift is uncertain at the  $\sim 0.4$  mag level in the  $K$ -band, which is a substantial source of uncertainty for interpreting the evolution of galaxy populations across time. Any possible evolution in the IMF, as suggested by several independent lines of evidence, will only exacerbate this problem. 4) Assuming a distribution of stellar metallicities within a galaxy, rather than a fixed value as is usually assumed, can yield important differences when considering bands blueward of  $V$ , but is not a concern for redder bands. Spectroscopic information may alleviate some of these concerns, though uncertainties in the stellar spectral libraries and the importance of non-solar abundance ratios have not yet been systematically investigated in the SPS context.

*Subject headings:* stars: evolution — galaxies: evolution — galaxies: stellar content

## 1. INTRODUCTION

The spatially-integrated UV, optical, and near-IR light of a galaxy contains a wealth of information regarding its physical properties. The spectrum of this light is governed principally by the star formation and metal enrichment histories of a galaxy in conjunction with stellar evolution and attenuation by interstellar dust. Combining these ingredients in order to predict the spectrum of a galaxy is known as stellar population synthesis (SPS), and has an extensive history (e.g. Tinsley & Gunn 1976; Tinsley 1980; Bruzual 1983; Renzini & Buzzoni 1986; Bruzual & Charlot 1993; Worthey 1994; Maraston 1998; Leitherer & Heckman 1995; Fioc & Rocca-Volmerange 1997; Vazdekis 1999; Yi 2003; Bruzual & Charlot 2003; Jimenez et al. 2004; Maraston 2005; Cid Fernandes et al. 2005; Ocvirk et al. 2006).

Sophisticated SPS models have allowed for an enormous body of work aimed at constraining physical parameters of galaxies by comparing the observed spectroscopic and/or photometric properties of  $z \sim 0$  galaxies to SPS models. Physical parameters that are constrained by SPS include, but are not limited to, stellar masses (e.g. Bell et al. 2003; Kauffmann et al. 2003a; Panter et al. 2007), star formation

histories and rates (e.g. Kauffmann et al. 2003b; Panter et al. 2007), and metallicities (e.g. Gallazzi et al. 2005). SPS is now routinely used not only at  $z \sim 0$  but also at higher redshifts in order to interpret the observed broad-band colors and spectra of galaxies (e.g. Shapley et al. 2005; Daddi et al. 2007; Kriek et al. 2006; Bundy et al. 2006).

Key aspects of stellar evolution theory — an essential ingredient of any SPS model — have been extensively tested against observations including globular clusters and star counts in the solar neighborhood, stellar halo, and the Large and Small Magellanic Clouds (LMC and SMC, respectively), suggesting that in many respects they are sufficiently reliable to be applied in SPS modeling of observed galaxies. However, there are significant phases in stellar evolution that are still not well understood, both observationally and theoretically. Such phases include blue stragglers (BSs), the horizontal branch (HB), the asymptotic giant branch (AGB), and thermally pulsating AGBs (TP-AGBs). Relatedly, the different evolutionary path(s) taken by binary systems, which appear to constitute the majority of all stellar systems, is not well-understood. These phases are particularly important for SPS models because stars in such phases are more luminous than the main

sequence (in some cases by several orders of magnitude), and in the case of AGBs they can dominate the red/IR light in some age ranges of a coeval set of stars, while in the case of the HB and BS they can contribute importantly to the blue and UV light. These uncertainties will thus impact our ability to derive physical properties of galaxies (e.g. Charlot et al. 1996; Charlot 1996; Yi et al. 2003; Lee et al. 2007).

The potential importance of uncertain phases of stellar evolution was highlighted recently by the different treatments of TP-AGBs in the SPS models of Maraston (2005) and Bruzual & Charlot (2003). These models, when applied to high-redshift galaxies where light is dominated by  $\sim 0.2 - 2$  Gyr old populations, result in *systematic* factors of  $\sim 2$  differences in mass and age (Maraston et al. 2006; Bruzual 2007; Kannappan & Gawiser 2007). This example demonstrates the need for understanding in detail how the uncertainties in stellar evolution propagate into estimates of physical properties of galaxies.

In addition to uncertainties in stellar evolution, there are also substantial uncertainties in our knowledge of the stellar initial mass function (IMF Kroupa 2001). The IMF effects not only the normalization of the mass-to-light ratio but also, to a lesser degree, the colors of a coeval set of stars (Tinsley 1980). The IMF thus plays an important role in deriving physical properties of galaxies (e.g. Papovich et al. 2001; Lee et al. 2004). The IMF also controls the rate of luminosity evolution for a passively evolving system, and is thus of fundamental importance for interpreting the evolution of galaxy populations across time (e.g. Tinsley 1980; Yi et al. 2003).

In this paper we present a new SPS code that was developed in order to address the impact of uncertainties in stellar structure and evolution on the derived physical properties of galaxies. This new SPS model is then applied to a variety of galaxies drawn from the Sloan Digital Sky Survey (SDSS York et al. 2000) and the Two Micron All Sky Survey (2MASS Jarrett et al. 2000) at  $z \sim 0$ , and from a sample of luminous red galaxies at  $z \sim 2$ , in order to investigate the effects of uncertain phases of stellar evolution on derived physical properties such as stellar mass and star formation history. In addition to the uncertain aspects of stellar evolution, we also explore the effects of the IMF and the potential biases that arise when assuming a single metallicity for all stars in a galaxy rather than the more physical assumption of a distribution of stellar metallicities.

Where necessary, we adopt a flat  $\Lambda$ CDM cosmology with  $(\Omega_m, \Omega_\Lambda, h) = (0.26, 0.74, 0.72)$ . Throughout, mass-to-light ratios are quoted in units of  $M_\odot/L_\odot$ .

## 2. METHODS: FROM PHYSICAL PROPERTIES TO INTEGRATED LIGHT

### 2.1. Overview

This section describes the steps involved in SPS modeling. Briefly, the approach utilizes stellar evolution calculations from the zero-age main sequence to stellar death to generate isochrones, which are the age-dependent positions in the HR diagram of a coeval population of stars. A combination of empirical and empirically-calibrated theoretical stellar libraries are then used to assign a full spectrum to each point in the HR diagram. The resulting integrated light from a coeval set of stars (referred to as a ‘simple stellar population’, or SSP) is then simply a sum of all the spectra along an isochrone, weighted by the number of stars at a given stellar mass, i.e. the IMF. Finally, the integrated light from a galaxy with a complex star formation history (SFH) is a convolution

of a time-dependent SSP with the SFH and a prescription for attenuation by dust. These steps are described in detail in the following sections. The uncertainties associated with SPS modeling are explored in depth in §3.

### 2.2. Stellar evolution

The core of any SPS model is the stellar evolution tracks that allow one to follow the evolution of stars of any mass from the zero-age main sequence to later evolutionary stages. The tracks must be sufficiently well sampled in both mass and time so that isochrones can be constructed. Many groups have produced publically available libraries of stellar evolution models (e.g. Bertelli et al. 1994; Girardi et al. 2000; Cioni et al. 2006; Schaller et al. 1992; Cassisi et al. 2000; Yi et al. 2001; Dotter et al. 2007).

We make use of the latest set of models from the Padova group<sup>1</sup> (Marigo & Girardi 2007; Marigo et al. 2008). The library of isochrones includes stars with initial masses  $0.15 \leq M \leq 100 M_\odot$  spanning ages  $10^{6.6} < t < 10^{10.2}$  yrs, with outputs at equally spaced intervals of  $\Delta(\log(t/\text{yr})) = 0.05$ , and for metallicities in the range  $10^{-4} < Z < 0.030$ , in equally spaced intervals of  $\log(Z) = 0.1$ . In the following we adopt  $Z_\odot = 0.019$ . These isochrones include a detailed treatment of the TP-AGB phase that has been calibrated against near-IR data from the LMC and SMC. The Padova models are supplemented in the mass range  $0.10 \leq M < 0.15 M_\odot$  with the non-evolving stellar models of Baraffe et al. (1998). Stars at this low mass range neither evolve off the main sequence nor contribute significantly to the total light emitted from a galaxy. Nonetheless they contribute substantially to the total stellar mass of a galaxy.

### 2.3. Spectral libraries

In addition to accurate stellar evolution models, the SPS formalism also requires an extensive, well-calibrated spectral library. We make use of the semi-empirical BaSeL3.1 library (Lejeune et al. 1997, 1998; Westera et al. 2002), which is a compilation of model atmosphere calculations for a wide range in effective temperature and surface gravity, for the full range of metallicities in the Padova stellar evolution models. The library spans the wavelength range  $91 - 160 \mu\text{m}$  at a resolving power of  $\lambda/\Delta\lambda \approx 200 - 500$ . The library does not include stars hotter than 50,000 K. We approximate the spectra of such stars as pure blackbodies.

The original model atmosphere calculations have been recalibrated by coupling the libraries to theoretical isochrones and comparing to globular cluster color-magnitude diagrams for a range in metallicity (Westera et al. 2002). Corrections to the original atmospheric models are significant especially for  $M$  stars because the models do not include the important effect of line blanketing due to molecular lines. As discussed in detail in Westera et al. (2002), the BaSeL library cannot simultaneously match the color-magnitude globular cluster data and the observed  $UBVRIJHKL$  color-temperature relations for individual stars. It is not known whether the color-temperature relations or the theoretical isochrones are the source of the discrepancy. This implies that the stellar library itself suffers unknown systematic uncertainties because of the choice to calibrate the models against the globular cluster data.

The BaSeL3.1 stellar spectral library does not include the spectra of TP-AGBs. It is critical to include the spectra of

<sup>1</sup> The Padova isochrones are publically available on the web: <http://stev.oapd.inaf.it/cgi-bin/cmd>.

such stars since they dominate the light output of intermediate age stellar populations (Maraston 2005). We make use of average TP-AGB spectra compiled by Lançon & Mouhcine (2002) from more than 100 optical/near-IR spectra presented in Lançon & Wood (2000). The library spans the wavelength range  $0.5 - 2.5 \mu\text{m}$  and is separated into oxygen-rich and carbon-rich spectra. The O-rich and C-rich spectra are further divided into nine and five bins in  $I-K$  color, respectively.  $I-K$  color is then converted into  $T_{\text{eff}}$  with the theoretical metallicity-dependent color-temperature relations in Bessell et al. (1991).

It is important to note that the metallicity of the observed spectra in this library are not known. Lançon & Mouhcine (2002) assume that the stars are all approximately solar metallicity because approximately three quarters of the spectra are from the field of the Milky Way. The authors advocate extending the library to non-solar metallicities with the following prescription: take  $T_{\text{eff}}$  and  $Z$  from the stellar evolution models, use the color-metallicity-temperature relations of Bessell et al. (1991) to infer the  $I-K$  color, and then use the library spectrum that most closely matches that color. Moreover, the spectra are not binned as a function of luminosity (or surface gravity). Rather, it is assumed that the spectra are not sensitive to luminosity.

Both the empirically unknown luminosity and metallicity dependence of the spectra introduce significant uncertainties that are difficult to quantify. Rather than introduce parameters that can be varied to encompass the possible effects of these uncertainties, we take the following approach. The standard prescription mentioned above is utilized to assign spectra to TP-AGB stars. Any uncertainty in the conversion between theoretical quantities ( $L_{\text{bol}}$  and  $T_{\text{eff}}$ ) and the emergent spectra is incorporated into uncertainties in the theoretical quantities themselves, as discussed in §3.1. We take this approach because uncertainties in the theoretical quantities are highly degenerate with uncertainties in the relation between theoretical quantities and emitted spectra, so it is simpler to combine all uncertainties into the former.

Neither the spectral libraries nor the stellar evolution calculations used herein account for the possibility of non-solar abundance ratios. We return to this point in §6.4.

#### 2.4. The initial mass function

The initial distribution of stellar masses along the main sequence, known as the stellar initial mass function or IMF, has been studied extensively for decades (e.g. Salpeter 1955; Scalo 1986; Scalo et al. 1998; Kroupa 2001; Chabrier 2003). Of particular relevance for SPS is the logarithmic slope of the IMF, especially near  $\sim 1M_{\odot}$  for old stellar populations, and its possible universality (both in space and time). Direct measurements of the IMF in the Galaxy are extremely challenging (for extensive discussion of the difficulties see Scalo et al. 1998; Kroupa 2001, see also §3.4).

In order to explore the importance of the IMF, we adopt the form advocated by van Dokkum (2008):

$$\Phi \equiv \frac{dn}{d\ln M} = \begin{cases} A_l (0.5n_c m_c)^{-x} \exp\left[\frac{-(\log M - \log m_c)^2}{2\sigma^2}\right] & (M \leq n_c m_c) \\ A_h M^{-x} & (M > n_c m_c) \end{cases} \quad (1)$$

with  $A_l = 0.140$ ,  $n_c = 25$ ,  $x = 1.3$ ,  $\sigma = 0.69$ , and  $A_h = 0.158$ . Variation of the IMF is incorporated in the characteristic mass  $m_c$ . Throughout we adopt lower and upper mass cut-offs of  $0.1M_{\odot}$  and  $100M_{\odot}$ , respectively.

Equation 1 is almost identical to the form advocated by Chabrier (2003) for  $m_c = 0.08$ , and is also very similar to the piece-wise power-law IMF proposed by Kroupa (2001), again for  $m_c = 0.08$ . From fitting the color and luminosity evolution of cluster ellipticals van Dokkum (2008) suggests that  $m_c \sim 2$  at  $z \gtrsim 4$ . In §3.4 we discuss further the existing evidence for an IMF that evolves in time and discuss more generally the importance of the IMF in SPS modeling. Its importance in understanding galaxy evolution was first discussed in Tinsley (1980); we discuss its importance in a modern context in §6.2.

It has been known since the work of Tinsley (1980) that the logarithmic slope of the IMF at the main-sequence turn-off point determines the rate of luminosity evolution of a passively evolving system (for a system with ongoing star-formation it is the IMF in addition to the star formation history that determines the rate of luminosity evolution). For this reason it is important that the logarithmic slope of the IMF be continuous. Thus, while the IMF of Kroupa (2001), which is a piece-wise power-law, is similar in magnitude to other continuous IMFs, such as the one used herein, the continuous variety must be preferred since they do not introduce artificial jumps in the luminosity evolution of passive systems. This issue is especially acute since the Kroupa (2001) IMF changes logarithmic slope at  $1M_{\odot}$ , precisely the turn-off point for an old stellar population. We return to these issues in §3.4 and §6.2.

#### 2.5. SSPs

With the isochrones, composite spectral library, and IMF in hand, we are now in a position to construct SSPs, which are the building blocks of SPS modeling. The spectrum from a coeval set of stars of metallicity  $Z$  at time  $t$  after birth can be described as:

$$S(t, Z) = \int_{M_i^l}^{M_i^u} \Phi(M_i) \Lambda[L(M_i, Z, t), T(M_i, Z, t), Z] dM_i \quad (2)$$

where  $M_i$  is the initial (zero-age main sequence) mass,  $M_i^l$  and  $M_i^u$  are lower and upper mass cut-offs,  $\Phi$  is the IMF,  $\Lambda$  is a spectrum from the stellar library, and  $L$  and  $T$  are the bolometric luminosity and effective temperature of a star of mass  $M_i$  and metallicity  $Z$ . In the following we adopt  $M_i^l = 0.1M_{\odot}$ .  $M_i^u(t)$ ,  $L(t)$ , and  $T(t)$  are determined by stellar evolution.

The mass of a coeval set of stars is:

$$M(t) = \int_{M_i^l}^{M_i^u(t)} \Phi(M_i) M_{\text{evol}}(M_i) dM_i + M_{\text{rem}} \quad (3)$$

where  $M_{\text{evol}}(M)$  is the evolved mass of a star of initial mass  $M_i$  and  $M_{\text{rem}}$  is the amount of mass locked up in remnants including white dwarfs, neutron stars, and black holes.

We follow the prescription of Renzini & Ciotti (1993) in assigning remnant masses to dead stars: stars with initial masses  $M_i \geq 40M_{\odot}$  leave a remnant black hole of mass  $0.5M_i$ , initial masses  $8.5 \leq M_i < 40M_{\odot}$  leave behind a  $1.4M_{\odot}$  neutron star, and initial masses  $M_i < 8.5M_{\odot}$  leave a white dwarf of mass  $0.077M_i + 0.48$ . This prescription is standard in SPS (Maraston 1998; Bruzual & Charlot 2003), although clearly these relations are not known to great precision (see Catalán et al. 2008, for a recent summary of the constraints on the initial-final mass relation for white dwarfs). For most purposes the above prescription amounts to a normalizing factor in the mass-to-light ratio, and it is thus of little concern for the present work. However, if these relations depend on other

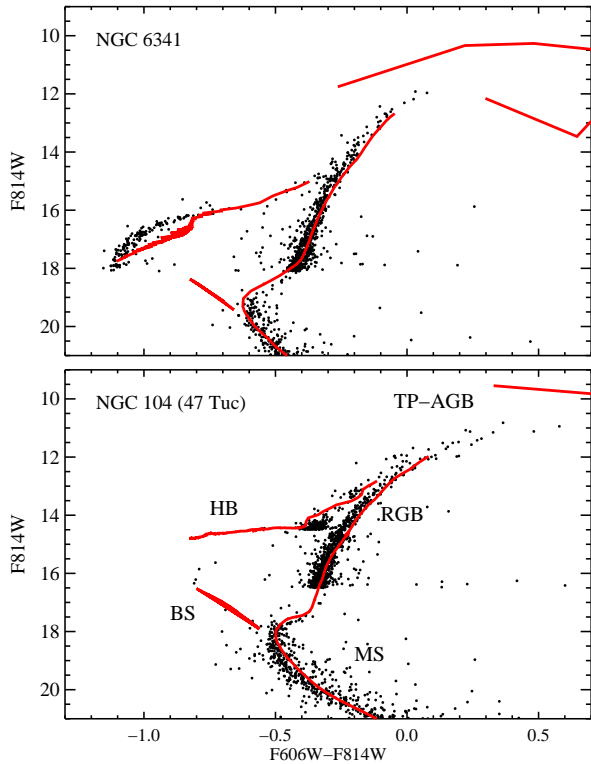


FIG. 1.— Observed CMD of two globular clusters from the *HST* (Brown et al. 2005) compared to our SPS model. The important evolutionary phases are labeled in the figure, including the main sequence (MS), blue stragglers (BS), the horizontal branch (HB), red giant branch (RGB), and the thermally-pulsating AGBs (TP-AGB). The lines are not a fit to the points; they are however similar in metallicity and age to the observed globular clusters and thus should adequately represent the data. In both panels only a fraction of the data is plotted below the RGB for clarity. *Top Panel:* NGC 6341 has an age of 14.5 Gyr and a metallicity of  $[\text{Fe}/\text{H}] = -2.14$  (Brown et al. 2005); the model has an age of 14.1 Gyr and a metallicity of  $[\text{Fe}/\text{H}] = -2.28$ . Notice the clear blueward extension of the HB, as is expected for metal-poor globular clusters. *Bottom Panel:* NGC 104 has an age of 12.5 Gyr and a metallicity of  $[\text{Fe}/\text{H}] = -0.7$  (Brown et al. 2005); the model has an age of 12.6 Gyr and a metallicity of  $[\text{Fe}/\text{H}] = -0.68$ .

parameters such as metallicity then they will have to be considered in greater detail.

### 2.6. Isochrone synthesis

The SSPs generated in the previous section describe the spectral evolution of a coeval set of stars. The final step in SPS modeling is to generate the time-dependent spectrum of a galaxy made of stars of varying ages. This flux arises from the following integral:

$$F(t) = \int_0^t \Psi(t-t') S_\nu(t', Z) e^{-\hat{\tau}_\lambda(t')} dt' \quad (4)$$

where  $\Psi$  is the star formation rate,  $S_\nu(t, Z)$  is an SSP at time  $t$  and metallicity  $Z$ , and  $e^{-\hat{\tau}_\lambda(t)}$  describes the attenuation of starlight by dust. Note that we assume that the metallicity is time-independent. This is a common approach in SPS modeling, though see Panter et al. (2007) who allow  $Z(t)$ .

The star formation rate is assumed to commence at some epoch  $T_{\text{start}}$ . We allow for star formation to be characterized by two components. One component is a constant level of star formation quantified as the fraction,  $C$ , of star formation occurring in this mode. The second component exponen-

TABLE 1  
SUMMARY OF SPS PARAMETERS

Parameter	Description	Range
$\Delta_T$	Shift in $\log(T_{\text{eff}})$ along the TP-AGB	$[-0.2, 0.2]$
$\Delta_L$	Shift in $\log(L_{\text{bol}})$ along the TP-AGB	$[-0.4, 0.4]$
$f_{\text{BHB}}$	Fraction of blue HB stars	$[0.0, 0.5]$
$S_{\text{BS}}$	Specific frequency of blue straggler stars	$[0, 10]$
$\tau$	SFR e-folding time (Gyr)	$[0, \infty)$
$C$	Fraction of mass formed in a constant mode of SF	$[0, 1]$
$T_{\text{start}}$	Age of Universe when SF commences (Gyr)	$[0.0, 5.0]^a$
$\hat{\tau}_1$	Extinction surrounding young stars	$[0, \infty)$
$\hat{\tau}_2$	Extinction surrounding old stars	$[0, \infty)$
$Z$	Stellar metallicity	$[0.0001, 0.030]$
$m_c$	Characteristic mass of the IMF	$[0.08, 2.0]$

<sup>a</sup> The upper bound on the value of  $T_{\text{start}}$  is set to  $T_{\text{univ}}$  for galaxies at a redshift where the age of the Universe is younger than 5 Gyr.

tially decreases with time and is characterized by the e-folding timescale  $\tau$ . Thus, for the star formation rate we have:

$$\Psi(t) = \frac{(1-C)}{\tau} \frac{e^{-t/\tau}}{e^{-T_{\text{start}}/\tau} - e^{-T_{\text{univ}}/\tau}} + \frac{C}{T_{\text{univ}} - T_{\text{start}}}, \quad T_{\text{start}} \leq t \leq T_{\text{univ}} \quad (5)$$

where  $\Psi$  is normalized such that one solar mass of stars is created over the age of the Universe,  $T_{\text{univ}}$ . Note that mass-to-light ratios do not depend on the normalization of the star formation rate since both the mass and light are integrals over  $\Psi$ . Our goal will be to determine the mass-to-light ratios of galaxies and then to multiply by the measured galactic light to infer the total stellar mass; our results will thus be entirely insensitive to this normalization of  $\Psi$ .

We adopt the simple two-component dust model of Charlot & Fall (2000), where  $\hat{\tau}(t)$  is given by

$$\hat{\tau}_\lambda(t) \equiv \begin{cases} \hat{\tau}_1(\lambda/5500)^{-0.7} & t \leq 10^7 \text{ yr} \\ \hat{\tau}_2(\lambda/5500)^{-0.7} & t > 10^7 \text{ yr} \end{cases} \quad (6)$$

In this model, the optical depth for young stellar systems is associated with dust in molecular clouds, in which the young stars are embedded. Following the disruption of molecular clouds, which occurs on a timescale of  $\sim 10^7$  yr (Blitz & Shu 1980), the optical depth is associated with a uniform screen across the galaxy. Charlot & Fall (2000) found that values of  $\hat{\tau}_1 \sim 1.0$  and  $\hat{\tau}_2 \sim 0.3$  adequately described an array of observational data. In the following these are left as free parameters. The wavelength-dependence was also constrained by the available data in Charlot & Fall (2000) although it too could be left as a free parameter. We leave it fixed for simplicity.

### 3. IMPORTANT UNKNOWNNS: STELLAR EVOLUTION, THE IMF, AND THE DISTRIBUTION OF STELLAR METALLICITIES

As discussed in the Introduction, there are numerous phases of stellar evolution that are not well understood on both theoretical and observational grounds. In this section we discuss three phases of particular importance: the TP-AGB, HB, and blue stragglers, and how these phases can effect the integrated light from a galaxy. These phases are important in SPS due to their high bolometric luminosity relative to the luminosity of main-sequence turn-off stars. There are additional phases that are not well understood, including post-AGB and Wolf-Rayet stars, that we will not discuss because they are thought to be important primarily in the UV and for very young populations, respectively — two observational regimes that we

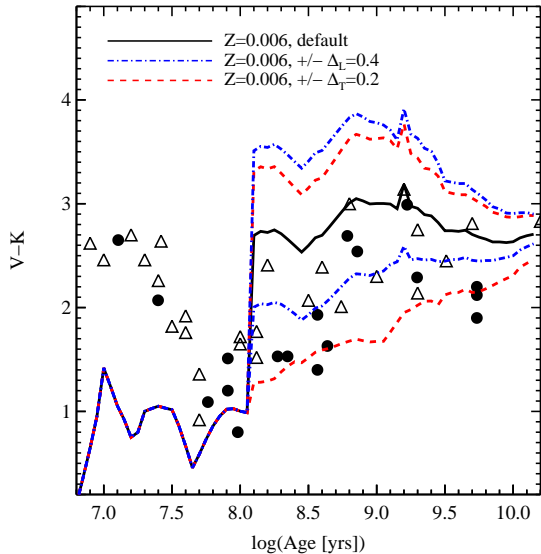


FIG. 2.—  $V-K$  colors of LMC star clusters as a function of cluster age. Data are from the compilations of Persson et al. (1983, *filled circles*) and Kyeong et al. (2003, *open triangles*). Ages for the Persson et al. (1983) sample are adopted from Girardi et al. (1995). The average metallicity of the LMC is  $Z \approx 0.006$  (Cioni et al. 2006). These data are compared to our default SPS model (*solid line*), and for a model with variations in the TP-AGB temperatures and luminosities by  $\pm 0.2$  dex and  $\pm 0.4$  dex (*dashed and dot-dashed lines*, respectively). Note that the standard stellar tracks without modification to the TP-AGB stars (*solid lines*) predict  $V-K$  colors redder than the majority of observed clusters.

will not address herein. In this section we also explore the importance of the IMF and the impact of assuming a distribution of stellar metallicities, rather than a single metallicity, on the derived properties of galaxies.

In order to guide the eye, in Figure 1 we plot the color-magnitude diagram (CMD) for two globular clusters observed with the *Hubble Space Telescope* (*HST*; Brown et al. 2005), and compare them to stellar evolution tracks for models with ages and metallicities comparable to the observed clusters. This figure highlights the locations of the various important phases of stellar evolution that will be discussed in the following sections.

### 3.1. Thermally-pulsating AGB stars

Thermally-pulsating AGB stars (TP-AGBs) are an extremely difficult phase of stellar evolution to model. The thermal pulses are thought to be driven by an instability arising when stars undergo helium shell burning. Hydrogen burning above the helium shell dumps helium ash into the helium burning shell, which increases the energy output of the helium shell. Since the helium shell is both thin and partially degenerate, the shell cannot readjust to the increased energy production, and a thermal runaway ensues until the star can readjust. This instability occurs in stars with initial masses  $\lesssim 5M_{\odot}$  and hence for stellar populations with ages  $\gtrsim 10^8$  years (Marigo et al. 2008).

As mentioned in the Introduction, the importance of this phase of stellar evolution recently became apparent when it was revealed that the SPS codes of Bruzual & Charlot (2003) and Maraston (2005) produce systematically different predictions for the masses and ages of intermediate age galaxies. It quickly became clear that the different treatment of TP-AGBs

in these models, which dominate the light in the near-IR for stellar populations several gigayears old, was the source of the difference (Maraston et al. 2006).

Progress in understanding the TP-AGB phase is hampered not only by the aforementioned difficulties in theoretical modeling but also by the lack of observations of stars in this phase. Observations are difficult because, while such stars are intrinsically luminous, they are also very rare due to the short amount of time stars spend in this phase. Due to their rareness, they are often not seen in star clusters, and thus the standard technique of comparing SSPs to observed globular clusters does not shed light on the TP-AGB phase (see e.g. Figure 1). The TP-AGB phase is best studied in the field of the Milky Way and in the LMC and SMC — regions where bright stars can be resolved in large numbers by ground-based telescopes. Appealing to data collected from such large regions introduces additional uncertainties, however, because the stars in such a sample span a range of ages and metallicities, neither of which are known.

The uncertainties associated with TP-AGB stars are modeled in the following manner: the location of the TP-AGB track (see e.g. Figure 1) in the HR diagram is specified by two parameters,  $\Delta_L$  and  $\Delta_T$ , that characterize the shift in  $\log(L_{\text{bol}})$  and  $\log(T_{\text{eff}})$ , respectively, with respect to the default tracks provided by the models of Marigo et al. (2008). For simplicity, these shifts are independent of time for an SSP.

This simple parameterization is motivated by the fact that several uncertain steps are required in order to transform a theoretical TP-AGB star into observable properties. First, its luminosity and temperature must be specified, as a function of metallicity, as given by stellar evolution calculations. Next, the luminosity, temperature, and metallicity must be converted to a full spectrum for the star. This step is made with observed spectra of a sample of TP-AGB stars (with unknown metallicities) since theoretical TP-AGB spectra are extremely difficult to calculate. Finally, reddening by circumstellar dust may be important, although our default models do not include this effect. Each of these steps carries significant uncertainties. Since we are only interested in transforming a theoretical TP-AGB star into observable properties, we have incorporated all of these uncertainties into the two parameters described above.

For example, if after fitting our model to an observed galaxy we find non-zero values for either or both of these parameters, then we would conclude that either our default stellar evolution model is inaccurate, or our stellar spectral library is flawed, or there is substantial circumstellar dust that we are not including, or some combination of all three of these.

While the details of the TP-AGB phase, and hence the values of the parameters  $\Delta_L$  and  $\Delta_T$  are uncertain, data from both the Milky Way and Magellanic Clouds provide valuable constraints on these uncertainties. Figure 2 plots the  $V-K$  color of star clusters as a function of cluster age for clusters from the LMC. Since each cluster is an SSP, this plot effectively shows the  $V-K$  evolution of a single SSP at the mean metallicity of the LMC, which is  $Z = 0.006$  (Cioni et al. 2006). This figure includes the SPS predictions for a standard model at  $Z = 0.006$ , and models where the parameters  $\Delta_T$  and  $\Delta_L$  and varied by  $\pm 0.2$  and  $\pm 0.4$ , respectively.

As noted in Marigo et al. (2008), the SSP rapidly reddens at  $t \approx 10^8$  years because the AGB phase occurs only in stars with masses less than  $M_i \sim 5M_{\odot}$ . Marigo et al. (2008) also note that this rapid reddening is stronger than observations al-

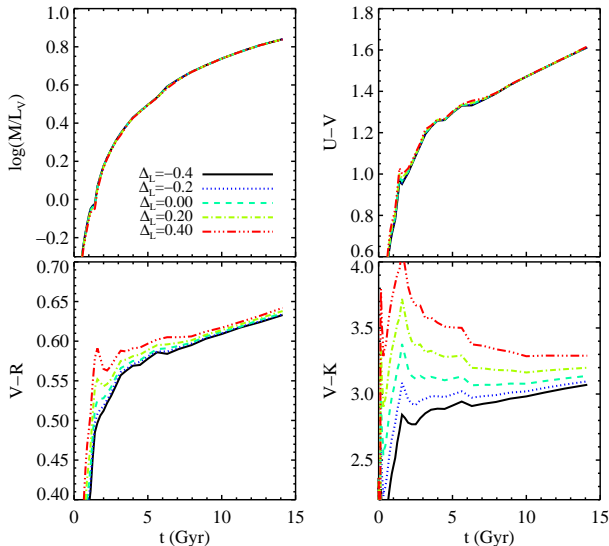


FIG. 3.— Evolution of SSPs at solar metallicity for a range in the parameter  $\Delta_L$ , the overall shift in  $\log(L_{\text{bol}})$  of the TP-AGB phase. Since TP-AGB stars are cool, varying  $\Delta_L$  primarily effects bands redward of  $R$ . The mass-to-light ratio in the  $V$ -band,  $M/L_V$ , and the  $U-V$  color are entirely insensitive to this parameter.

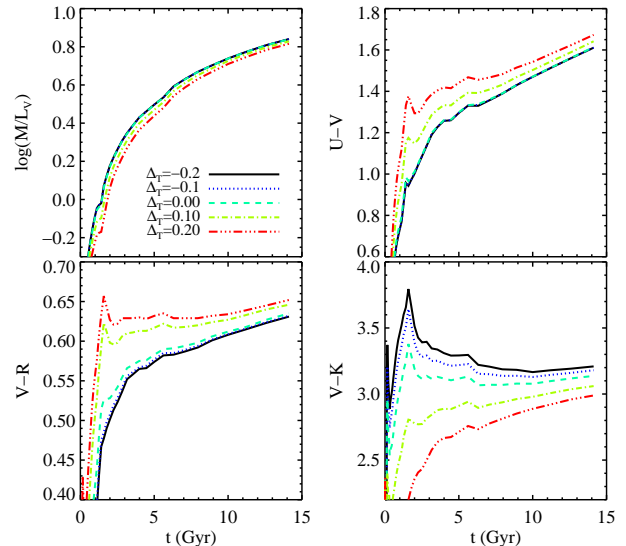


FIG. 4.— Same as Figure 3, except now the parameter  $\Delta_T$ , the overall shift in  $\log(T_{\text{eff}})$  of the TP-AGB phase, is varied. Increasing the temperature of the TP-AGB phase effectively shifts the dominant flux contribution of these stars from the  $K$ -band to bluer bands such as  $R$  and  $V$ . Thus hotter TP-AGBs can result in redder  $U-V$  colors as shown in the figure.

low, and they suggest that the source of the discrepancy lies in the treatment of mass-loss in the AGB phase. We mention in passing that the models of Maraston (2005) do not suffer from this effect (see Maraston 1998), in part because they were calibrated to fit the LMC star cluster data. At ages younger than  $10^8$  years the model predicts colors too blue compared to observations. Such young clusters are not thought to contain AGB stars; the discrepancy can thus not be attributed to the AGB phase. Marigo et al. (2008) offer a number of possible explanations for the mismatch between model and data but ultimately this mismatch must be accepted in the current generation of models.

Moreover, it is clear that the default models (where  $\Delta_L = 0.0$  and  $\Delta_T = 0.0$ ) predict  $V-K$  colors that are too red compared to the observed star clusters at  $t \gtrsim 10^8$  years. The figure shows that increasing the temperature of TP-AGB stars by 0.2 dex and/or decreasing their luminosity by 0.4 dex results in better agreement with the data. Models that decrease the temperature and/or increase the luminosity do not produce substantially worse agreement than the default model at late times ( $t \gtrsim 10^{9.5}$  years) but are much redder than the data for intermediate ages.

From this comparison we conclude that values for the TP-AGB parameters in the range  $-0.4 < \Delta_L < 0.0$  and  $0.0 < \Delta_T < 0.2$  cannot be ruled out by current data from the LMC. When fitting to observations we allow these parameters to vary in the wider range  $-0.4 < \Delta_L < 0.4$  and  $-0.2 < \Delta_T < 0.2$  for increased flexibility because these parameters may depend on metallicity in a way that could not be discerned from the comparison to the LMC.

The effects of  $\Delta_L$  and  $\Delta_T$  on the evolution of SSPs are explored more broadly in Figures 3 and 4, where the evolution of  $M/L_V$ ,  $U-V$ ,  $V-R$ , and  $V-K$  are plotted for a range of these TP-AGB parameters.

Figure 3 shows that it is primarily bands redward of  $V$  that are sensitive to  $\Delta_L$  — bluer bands are almost entirely insensitive to this parameter. This result is not surprising in light

of the fact that TP-AGB stars dominate the energy output redward of  $\sim 1 \mu\text{m}$ . It thus may be the case that the inclusion of near-IR information does not significantly reduce the errors in physical properties of galaxies, such as stellar masses, since the red light in galaxies is dominated by this uncertain phase of stellar evolution.

Figure 4 shows the impact of the  $\Delta_T$  parameter on the evolution of SSPs. This TP-AGB parameter has a strong influence on not only the  $V-K$  color but on bluer colors as well. Moreover, this parameter has opposite effects on  $V-K$  compared to  $U-V$  and  $V-R$  colors, in the sense that  $\Delta_T > 0$  results in bluer  $V-K$  colors and redder  $U-V$  and  $V-K$  colors. This trend is due to the fact that hotter TP-AGB stars emit most of their light in progressively bluer bands compared to cooler TP-AGB stars. So as  $\Delta_T$  is increased, the integrated flux in the  $V$ - and  $R$ -bands is increased at the expense of redder bands such as  $K$ .

These TP-AGB parameters will be included in our fits to observed broad-band photometry of galaxies in §5.

### 3.2. Horizontal branch stars

The horizontal branch (HB) consists of old low-mass ( $M \lesssim 1M_{\odot}$ ) stars burning helium in their cores, and hydrogen in a shell surrounding the core, at nearly constant bolometric luminosity (Sweigart 1987; Lee et al. 1990, 1994). The narrow range of luminosities is driven largely by the constant core He mass of stars that enter the HB phase.

The temperature of HB stars has received extensive attention in the literature, in part because HB stars are luminous and thus accurate knowledge of their temperatures is important for modeling the integrated light from a galaxy. Observationally, it appears that metal-rich globular clusters contain almost exclusively red HB stars, while HB stars in metal-poor clusters ( $[\text{Fe}/\text{H}] \lesssim -1.4$ ) populate a wide range of temperatures (Harris 1996). This trend is thought to be due to metallicity-dependent mass-loss on the RGB, which leads to a smaller envelope mass in metal-poor compared to metal-rich systems, and hence hotter HB stars (Greggio & Renzini

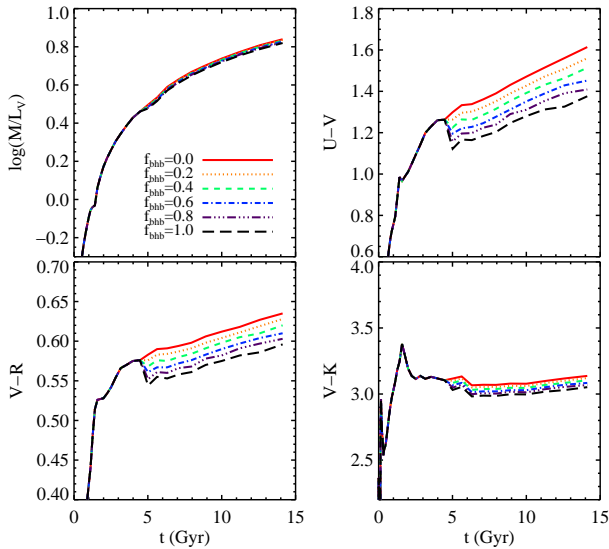


FIG. 5.— Same as Figure 3, except now the parameter  $f_{BHB}$ , the fraction of blue HB stars, is varied. In our model this parameter is turned on at  $t = 5$  Gyr, as is clear from the figure, because there are no observed globular clusters with a blue horizontal branch and an age of less than 5 Gyr. Blue HB stars are hot; increasing their fraction thus has the largest impact on bluer colors such as  $U - V$  and  $V - R$ , and a smaller effect on  $V - K$ .

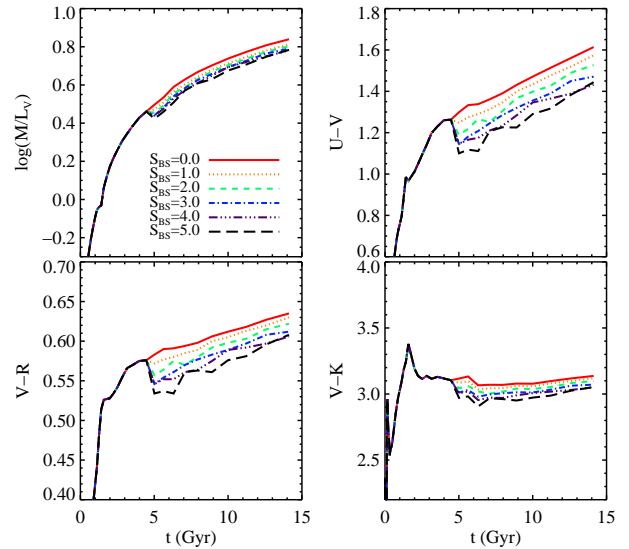


FIG. 6.— Same as Figure 3, except now the parameter  $S_{BS}$ , the specific frequency of blue stragglers, is varied. In our model this parameter is turned on at  $t = 5$  Gyr, as is clear from the figure. The impact of BS stars is qualitatively similar to but smaller in magnitude than blue HB stars because BS stars are at roughly the same temperature as blue HB stars but are nearly an order of magnitude less luminous (see Figure 1).

1990). One of the fundamental problems with understanding the morphology (i.e. temperature distribution) of the HB is that the temperature of HB stars is extremely sensitive to the amount of mass lost. For example, a difference in envelope mass of only  $0.04M_{\odot}$  can correspond to a temperature increase from 5,000 K to 11,000 K (Rich et al. 1997), a temperature increase sufficient to explain the morphology of metal-poor systems. Since an adequate theory of mass-loss for evolved stars does not exist, understanding the morphology of the HB from first principles is extremely challenging.

One might hope to understand the HB morphology purely observationally and thereby assess its potential impact on SPS without the aid of theoretical models. This approach has also proved difficult. In particular, there are clear examples of metal-rich star clusters with a blue HB (Rich et al. 1997; Brown et al. 2000; Kalirai et al. 2007), suggesting that the morphology of the HB may not depend only on metallicity. On the other hand, data from the *Hipparcos* satellite demonstrate that there is not a significant population of blue HB stars in the solar neighborhood (Jimenez et al. 1998). This may be attributed to the paucity of metal-poor stars in the solar neighborhood (Rana 1991). However, we might expect other galaxies, especially ellipticals, to contain a significant population of metal-poor stars because recent galaxy formation models imply that ellipticals form their stars in a manner closely analogous to the closed-box model. Indeed SPS modeling of the spectra of local elliptical galaxies suggests that  $\sim 5 - 20\%$  of the stellar mass in such galaxies may be associated with metal-poor stars (Worthey et al. 1996; Maraston & Thomas 2000; Trager et al. 2005; Maraston et al. 2009).

Blue HB stars are an important phase of stellar evolution to understand because they can strongly effect the balmer lines (e.g. Lee et al. 2000), and can complicate the estimation of quantities such as stellar age and metallicity (e.g. Lee et al. 2002). With sufficient spectral resolution and signal-to-noise, the spectral signatures of a blue HB can in fact be isolated (Trager et al. 2005). However, for broad-band colors and low

signal-to-noise data, it is difficult to make this distinction.

Despite these large observational and theoretical uncertainties, some SPS codes do not include blue HB stars (Bruzual & Charlot 2003), or, if they are included, they are included only in metal-poor systems (Jimenez et al. 2004). Only the Maraston (2005) model includes blue HB stars at both low and high metallicity. We feel that the uncertainties in our knowledge of the HB warrant a more flexible treatment of the HB than is typically implemented.

To this end, in our SPS model we allow for a specified fraction of HB stars that are spread uniformly in temperature from the standard red end of the HB to 10,000 K *for the full range of metallicities we consider*. We refer to these HB stars with temperatures hotter than the red clump as blue HB stars. These blue HB stars are added for populations older than 5 Gyr. No globular clusters have been found with both younger ages and a blue HB morphology. Atlee et al. (2009) have recently shown that the UV excess in luminous early-type galaxies does not evolve appreciably since  $z \approx 0.65$ , suggesting that, if the UV excess is due to blue HB stars, then it is reasonable to assume a non-evolving blue HB for stellar populations older than several gigayears.

The bolometric luminosity of HB stars is left unaltered because, as stated above, their luminosities are understood both observationally and theoretically. The weight assigned to blue HB stars is a free parameter and is specified as the fraction of HB stars that are in this blue component,  $f_{BHB}$ . This parameter is allowed to vary from  $0 < f_{BHB} < 0.5$ . The upper limit is arbitrary but is motivated by the consideration that a galaxy with 20% of its stellar mass in metal-poor stars and a blue HB population in 40% of its metal-rich systems would have  $f_{BHB} = 0.5$ . Observationally, Dorman et al. (1995) infer from the UV upturn in elliptical galaxies that between 5–20% of HB stars are very blue. One might expect this fraction to increase as the overall metallicity of a galaxy decreases.

Figure 5 shows the color and  $M/L$  evolution of SSPs at solar metallicity for a range in the parameter  $f_{BHB}$ . The bluer col-

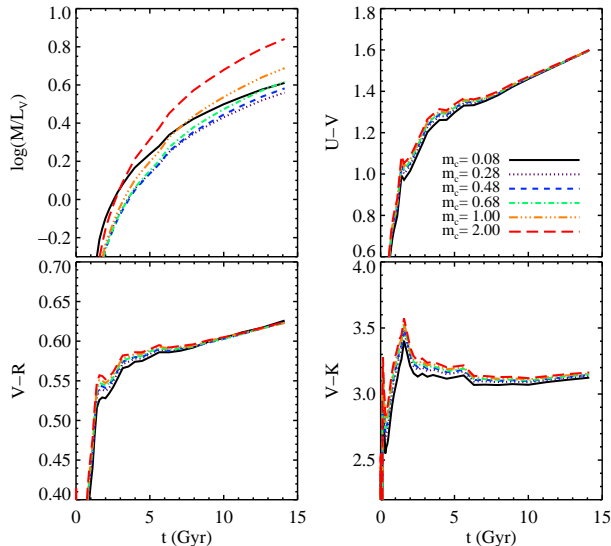


FIG. 7.— Same as Figure 3, except now the parameter  $m_c$ , the characteristic mass of the IMF, is varied. As discussed in the text, the IMF has a much larger influence on the luminosity evolution, and hence  $M/L$ , than color evolution. Nonetheless, IMF differences can induce color changes of order 0.1 mags in the near-IR at intermediate ages.

ors are more sensitive to this parameter than the redder colors. The addition of blue HB stars, in our implementation, does not significantly alter the evolution of colors at late times, but rather it amounts to an approximately constant blueward offset.

### 3.3. Blue straggler stars

As indicated in Figure 1, blue stragglers (BSs) are stars that extend blueward and brighter than the main sequence turn-off point. They are a ubiquitous feature of observed globular clusters (e.g. Sandage 1953; Bailyn 1995; Brown et al. 2005; Sarajedini et al. 2007). Their origin remains a mystery. Standard explanations are that BSs are either due to primordial binary evolution (McCrea 1964) or collisional merging (Bailyn 1995). If the later is in fact dominant then one expects BSs to have a negligible effect on the integrated light from a galaxy because collisions are only important at the high densities found in globular clusters, in which only a small fraction of galactic stellar mass is found. If binary evolution, due e.g. to mass transfer and/or coalescence, is responsible, then they may be common throughout galaxies due to the high primordial binary fraction of field stars of spectral type  $\sim K$  or earlier (Duquennoy & Mayor 1991; Lada 2006). Observations seem to suggest that both processes are at work in globular clusters (Davies et al. 2004; Piotto et al. 2004).

There are also some observational indications that BSs are factors of several more common in the field compared to globular clusters (Preston & Sneden 2000). There are several ways of explaining such a difference between field and cluster, but it is sufficient for our purposes to note that their observational status is sufficiently unconstrained to include BSs in our SPS modeling in a flexible way.

Turning to their observational consequences, Li & Han (2009) have incorporated the effects of binary star interactions into their SPS code and find that including binaries can result in broad-band colors bluer by  $\sim 0.05$  mags. Xin & Deng (2005) find that BSs in old open clusters can contribute as much as  $\sim 0.2$  magnitudes to the  $B-V$  color of the integrated

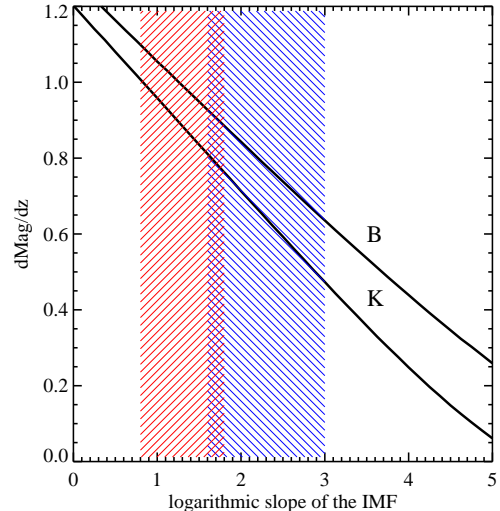


FIG. 8.— Change in magnitude per unit redshift at  $z \leq 1$  for a passive stellar population, as a function of the logarithmic slope of the IMF. Magnitude evolution in both the  $B$ - and  $K$ -bands are included. The hatched regions denote the uncertainties in the measured IMF slope at  $0.08 < M < 0.5M_{\odot}$  (left) and  $M \geq 1.0M_{\odot}$  (right; Kroupa 2001). Since luminosity evolution is determined by the IMF slope at the mass where stars are just leaving the main sequence, passive evolution is determined by the slope at  $\approx 1M_{\odot}$  for old ( $t \gtrsim 10^{10}$  yrs) stellar populations. In the  $K$ -band, the uncertainty in the IMF slope at  $1M_{\odot}$  translates into an uncertainty in  $dM/dz$  of  $\sim 0.4$  mags for an old, passively evolving stellar population.

cluster. They find no correlation between the number of BSs and the cluster age, suggesting that BSs may be a relatively stable phenomenon (though see discussion in Davies et al. 2004).

BSs are included in our SPS code with the following prescription. As with the blue HB stars, the BS phenomenon is ‘turned on’ for ages greater than 5 Gyr. Observationally, the specific frequency of BSs,  $S_{BS}$ , is defined as the number of BSs per unit HB star, i.e.  $S_{BS} \equiv N_{BS}/N_{HB}$ . Typical values for globular clusters are in the range  $0.1 < S_{BS} < 1$  (Piotto et al. 2004), although Preston & Sneden (2000) suggest that  $S_{BS}$  could be as high as five in the field. BSs typically are found in a region parallel to the zero-age main sequence starting at  $\sim 0.5$  mags brighter than the turn-off point and extending another  $\sim 2$  mags brighter (Xin & Deng 2005). In our code BSs populate a region from 0.5–2.5 mags brighter than the zero-age main sequence. The BS population is parameterized with the single free parameter  $S_{BS}$ .

Figure 6 shows the effect of BSs on the integrated colors and  $M/L$  of a solar metallicity SSP. BSs contribute mostly to the blue bands and at the  $\sim 0.1$  mag level, consistent with both models (Li & Han 2009) and observations (Xin & Deng 2005). BSs have less of an effect than HB stars because they are roughly an order of magnitude less luminous (cf. Figure 1).

### 3.4. The IMF

The IMF is very uncertain at masses  $0.8 \lesssim M \lesssim 2M_{\odot}$  because at these masses IMF constraints derived from field stars in the solar neighborhood rely on large and uncertain stellar evolution corrections (Kroupa 2001). While the IMF is also uncertain at both higher and lower stellar masses, this mass



range is critical for galaxies made of old ( $\gtrsim 10^9$  years) stars because the main-sequence turn-off of such old populations is  $\sim 1M_{\odot}^2$ , and, as discussed in §2.4, it is the logarithmic slope of the IMF at the main-sequence turn-off point that determines the rate of luminosity evolution for a passively evolving system. More generally, the observed IMF must be corrected for a large number of systematics including the fraction of binary stars, shot noise, and dynamical evolution, in order to infer the ‘true’ underlying single-star IMF. These corrections are large and uncertain.

While direct measurements of the IMF in the Galaxy are challenging, they are all but impossible in external galaxies beyond the LMC and SMC. This unfortunate situation is unlikely to improve. Nonetheless, much work has gone into constraining the IMF via indirect approaches. For example, evolution with redshift of  $M/L_B$  and  $U-V$  for galaxies on the fundamental plane suggests that the IMF may be weighted toward higher masses at  $z \sim 2$  compared to local measurements (van Dokkum 2008). Furthermore, comparison of the evolution of the cosmic star formation rate density, which is sensitive to the high-mass end of the IMF, to evolution of the cosmic stellar mass density, which is sensitive to the lower-mass end, also suggests that the IMF is different at  $z > 1$ , in the same sense as implied by the evolution of the fundamental plane (e.g. Hopkins & Beacom 2006; Davé 2008; Wilkins et al. 2008). Carbon-enhanced metal poor-stars also point toward a top-heavy IMF at early times (Lucatello et al. 2005; Tumlinson 2007a,b). These arguments are indirect, and should thus be treated with caution. However, in support of these conjectures, simple theoretical arguments suggest that the characteristic temperature of molecular clouds may be higher at earlier epochs, which in turn would lead to a higher Jeans mass and thus potentially a different IMF at early times (Larson 1998, 2005). For a review of evidence suggesting a varying IMF, see Elmegreen (2009).

In standard implementations of SPS the IMF is typically treated as an uninteresting overall normalization of the galactic stellar mass. This assumption is problematic for at least two related reasons as demonstrated in Figure 7, and first pointed out by Tinsley (1980). On the one hand, the IMF determines the relative weights to be assigned to various portions of the isochrones. If broad-band colors are dominated by one phase of stellar evolution, for example the main sequence turn-off, then they will be entirely insensitive to the IMF. This is approximately the case for the  $U-V$  color in Figure 7. However, if at least some colors are determined by a mixture of stellar evolutionary phases, such as the RGB and AGB phases, then these colors will be sensitive to the IMF, as seen in the  $V-K$  color in the figure (see also Maraston 1998).

This uncertainty in the colors due to the uncertainty in the IMF should arguably be included in SPS models because observational quantities are affected. Different IMFs can yield different colors which in turn will result in different predictions for ages and metallicities of galaxies. This can be contrasted with the effect of the IMF on the stellar mass of galaxies because there variation in the IMF leads only to an overall re-scaling of the stellar mass. See Westera et al. (2007) for a discussion of these effects and the prospects for constraining the form of the IMF from broad-band photometry of external galaxies. In the present work we do not marginalize over un-

certainties in the IMF when fitting the photometry of observed galaxies.

The second issue is that, even if colors are only mildly affected, the rate of luminosity evolution is strongly related to the logarithmic slope of the IMF, as shown in the top left panel of Figure 7. So while the stellar mass of galaxies *at a fixed epoch* may be relatively robust against IMF variations, in the sense that changing the IMF will change the stellar mass of all galaxies by the same relative amount, luminosity evolution is very sensitive to the IMF. The slope of the IMF near  $1M_{\odot}$  is not known to better than  $\pm(0.3-0.7)$  in the solar neighborhood (Kroupa 2001), and thus this is an important uncertainty to consider even if one wants to retain the notion of a universal IMF. This uncertainty makes it extremely difficult, for example, to interpret evolution in the luminosity function of bright galaxies in terms of a constraint on their stellar growth.

This point is demonstrated explicitly in Figure 8, where we plot the best-fit linear slope for the evolution of the absolute magnitude of an SSP with redshift, over the interval  $0 < z < 1$ , as a function of the logarithmic IMF slope. As mentioned above, for old stellar populations the main sequence turn-off mass is  $\sim 1M_{\odot}$ , and it is the slope of the IMF at the turn-off mass that is important for passive luminosity evolution. The figure demonstrates that passive fading of a population of stars since  $z = 1$  is uncertain at the  $\sim 0.4$  mag level in the  $K$ -band (see also Yi et al. 2003). In light of this effect, precise conclusions made from evolving luminosity functions (e.g. Wake et al. 2006; Brown et al. 2007; Cool et al. 2008) must be treated with extreme caution. See §6.2 for a detailed discussion of this issue.

### 3.5. Metallicity distributions

The stars within a galaxy do not form from gas at a single metallicity. Rather, if stars form from a ‘‘closed-box’’ of gas, where no inflow or outflow takes place, the metallicity distribution of the stars approaches:

$$\frac{dn}{d\ln Z} \propto Z e^{-Z/p} \quad (7)$$

where  $p$  is the true yield (Searle & Sargent 1972; Pagel 1997). It has been known for some time that the closed-box model predicts too many metal-poor stars in the solar neighborhood — the so-called G-dwarf problem (Rana 1991). A possible explanation is that gaseous inflow and/or outflow has been important in the formation of stars in the solar neighborhood (Larson 1972). Such an explanation is particularly attractive in the context of hierarchical structure growth, which is a robust feature of a universe dominated by cold dark matter.

In spite of the failure of the closed-box model at describing the solar neighborhood, one might expect it to fair better at describing the metallicity distribution of stellar populations formed over short time-scales. In such populations gaseous inflow and/or outflow are less important because they have less time to effect the metal content of the gas out of which stars are forming. Indeed, the metallicity distribution of stars in the bulge of the Milky Way can be somewhat better-described by a closed-box model with a yield of  $p = 0.015$ , although even in the bulge there appears to be too few metal-poor stars (Rich 1990; Zoccali et al. 2003). Inclusion of the metal-poor halo in the accounting may yet produce better agreement with the closed-box model. The paucity of metal-poor stars in comparison to the predictions of the closed-box model is evident in other galaxies as well (Worthey et al. 1996, 2005).

<sup>2</sup> The main-sequence turn-off mass decreases very slowly with time for old stellar populations. For example, at  $t = 10^9, 5 \times 10^9$ , and  $10^{10}$  years the turn-off mass is 2.0, 1.2, and  $1.0M_{\odot}$ , respectively.

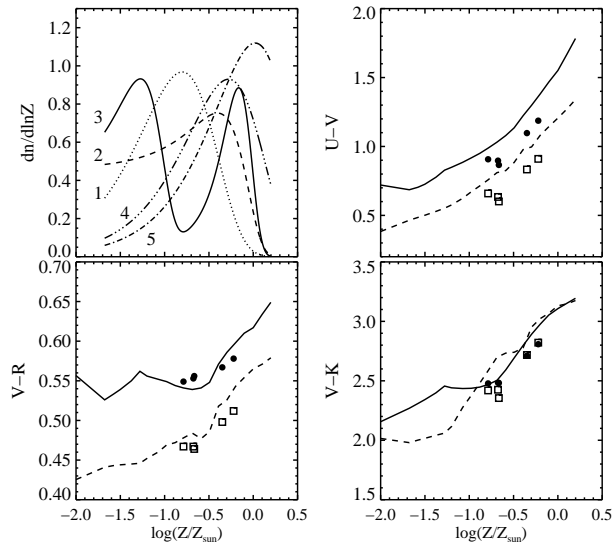


FIG. 9.— Effect of stellar metallicity on the evolution of an SSP. This figure compares the effect of a *distribution* of metallicities on the colors of SSPs to the colors of single-metallicity SSPs. Five metallicity distributions are shown in the top left panel. The colors of SSPs with such metallicity distributions are shown in the remaining three panels at  $t = 3.2$  (*open squares*) and 12.6 Gyr (*filled circles*), as a function of the mean metallicity of the distribution. These results are compared to the colors of single-metallicity SSPs as a function of metallicity, at 3.2 (*dashed lines*) and  $t = 12.6$  Gyr (*solid lines*). The distributions in the upper left panel are numbered according to their mean metallicities, in ascending order. Notice that the difference between the points and lines is small for colors redward of the  $V$ -band but are noticeable and systematic for  $U-V$ . See the text for details.

While it is clear that there are fewer observed metal-poor stars compared to the closed-box model, the stars constituting galaxies nevertheless have a distribution of metallicities and this fact is not included in standard SPS modeling. In order to explore the effects of a distribution of metallicities on the colors of SSPs, we consider three closed box models described by Equation 7 with  $p = 0.003, 0.010, 0.020$ , and two more flexible distributions that are the sum of two Gaussians:

$$\frac{dn}{d\ln Z} \propto e^{-(Z-\mu_1)^2/\sigma_1^2/2} + e^{-(Z-\mu_2)^2/\sigma_2^2/2} \quad (8)$$

where  $(\mu_1, \sigma_1^2, \mu_2, \sigma_2^2) = (0.010, 0.005, 0.005, 0.005)$  and  $(0.013, 0.003, 0.0005, 0.001)$ . In light of the discussion above, these distributions almost certainly contain more metal-poor stars than observations demand, and so they should be thought of as extreme scenarios for the metallicity distributions in real galaxies. Note also that we are assuming that metallicity and stellar age are uncorrelated. Of course, the mean metallicity of a galaxy will tend to increase with time and so one might expect younger stars to be more metal rich, on average, than older stars. Investigating constraints on the metallicity evolution of a galaxy will be the subject of future work.

The five metallicity distributions are shown in the top left panel of Figure 9. In the remaining panels of this figure we plot the dependence of the  $U-V$ ,  $V-R$ , and  $V-K$  colors on metallicity at two stellar ages. The colors as a function of single-metallicity SSPs (*lines*) are compared to the colors from the multi-metallicity stellar populations described above (*symbols*). Colors from the multi-metallicity populations are plotted against the average metallicity of the population. For the  $V-R$  and  $V-K$  colors there is no significant difference

between a single-metallicity SSP and a multi-metallicity SSP with the same average metallicity. Since we have chosen rather extreme metallicity distributions, this implies that the optical and near-IR colors shown here are entirely insensitive to the range of metallicities in a galaxy.

For the  $U-V$  color the multi-metallicity populations are  $\sim 0.1$  magnitudes bluer when compared to single-metallicity SSPs. The impact of a distribution of metallicities on the inferred color is comparatively strong for  $U-V$  because this color varies strongly, and non-linearly, with metallicity. We have found that this discrepancy between single and multi-metallicity populations increases into the ultraviolet (see also Schiavon 2007). We leave a more detailed discussion of this effect for future work, but note here that this difference could potentially lead to a mis-estimation of either/both the metallicity and age of a galaxy.

Recall that we have decoupled metallicity and horizontal branch morphology. As noted in §3.2, metal-poor globular clusters have extended horizontal branches, while metal-rich clusters have exclusively red horizontal branch stars. This can certainly produce a substantial difference between a single metallicity and multi-metallicity population of stars. Since we consider the horizontal branch morphology separately herein, we do not include its effect in this section. We have decoupled metallicity from horizontal branch morphology because, as discussed in §3.2, the dependence of the horizontal branch on metallicity is poorly understood.

### 3.6. Summary of important unknowns

In this section we have explored several important and yet uncertain ingredients in SPS modeling. These include uncertain phases of stellar evolution such as the TP-AGB stars, horizontal branch, and blue stragglers, the IMF, and the universal assumption in SPS modeling that every star in a galaxy has the same metallicity.

As Figures 3, 4, 5, and 6 show, the uncertain phases of stellar evolution can have a large effect on the color of an SSP within the plausible range of uncertainties. These uncertainties thus must be incorporated into any SPS model in order to derive accurate and robust physical parameters of galaxies.

Figures 7 and 8 show that the variations in the logarithmic slope of the IMF has a minor effect on the colors of an SSP but has a large effect on its luminosity evolution. This uncertainty must thus be incorporated whenever one attempts to discuss the luminosity evolution of galaxies.

Finally, Figure 9 compares the effect of assuming a single metallicity to a distribution of metallicities on the evolution of an SSP. The relation between color and average metallicity is essentially independent of the distribution of metallicities one assumes for bands redward of  $V$ . At bluer wavelengths the difference between single and multi-metallicity populations becomes more apparent. This effect, if not included in SPS models, may introduce unknown systematics. We will investigate this aspect in future work.

### 3.7. Comparison to other SPS models

In this section we compare our SPS model to two previous, highly used, models. Figure 10 shows the luminosity and color evolution of a solar metallicity SSP for our default model and the models of Bruzual & Charlot (2003, BC03) and Maraston (2005, M05). Also included in the figure are two predictions of our model with the TP-AGB parameters set to  $\Delta_L = -0.4$  and  $\Delta_T = 0.2$ . The M05 model predicts that the

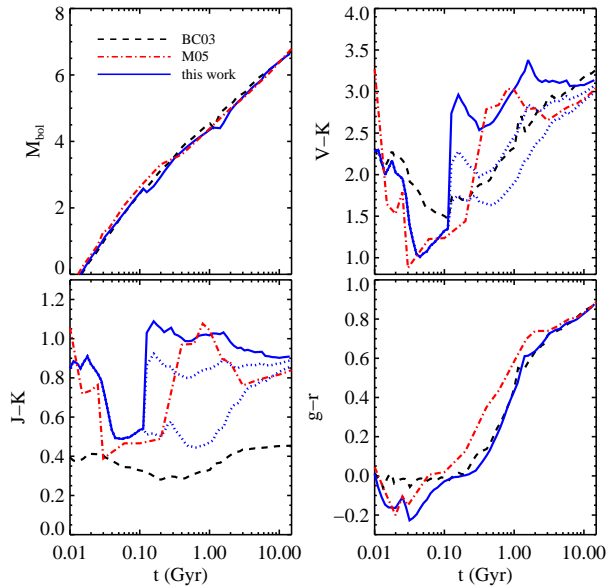


FIG. 10.— Comparison of the Bruzual & Charlot (2003, B03) and Maraston (2005, M05) SPS models to the default model presented herein for a solar metallicity SSP. We also include results of our model with  $\Delta_L = -0.4$  (upper dotted line) and  $\Delta_T = 0.2$  (lower dotted line) in the panels where these parameter choices result in noticeably different model predictions.

TABLE 2  
DEFINITION OF SDSS SAMPLES

Description	Luminosity Cut	Color Cut
bright red	$-24.0 < M_r - 5\log(h) < -22.0$	$0.70 < (g-r) < 0.90$
faint red	$-20.5 < M_r - 5\log(h) < -20.0$	$0.70 < (g-r) < 0.90$
bright blue	$-21.5 < M_r - 5\log(h) < -21.0$	$0.20 < (g-r) < 0.66$
faint blue	$-20.5 < M_r - 5\log(h) < -20.0$	$0.20 < (g-r) < 0.66$

NOTE. — All samples are within the redshift range  $0.10 < z < 0.12$ .

TP-AGB stars constitute a much larger fraction of the near-IR light compared to BC03. This explains the much redder  $J-K$  and  $V-K$  colors, and the redder  $g-r$  colors for  $t \lesssim 2$  Gyr shown in Figure 10.

Our default SPS model compares favorably with the M05 model, which is not surprising because our isochrones include TP-AGB calculations of a sophistication comparable to that in M05. In addition, our code is flexible enough to roughly capture the trends predicted by BC03. In the figure it is clear that the  $V-K$  color evolution of our model appears similar to BC03 when we set  $\Delta_L = -0.4$ . In other words, when we force the TP-AGB stars to be less important to the integrated SSP, our model converges to the BC03 model. This is one of the advantages of the flexible SPS model presented herein compared to others in the literature — the flexible model does not put priors on uncertain physics in stellar evolution. Instead, the model lets the data decide what parameters are most favored.

#### 4. DATA, AND DATA FITTING

We now turn to the task of fitting our SPS model to the photometry of galaxies. In this section we describe the data used and the details of the fitting procedure. In the following section we present the results.

#### 4.1. Data at $z \sim 0$

The Sloan Digital Sky Survey (SDSS; York et al. 2000; Abazajian et al. 2004; Adelman-McCarthy et al. 2006) is an extensive photometric and spectroscopic survey of the local Universe. As of Data Release 4 (DR4), imaging data exist over  $6670 \text{ deg}^2$  in five band-passes,  $u, g, r, i,$  and  $z$ . Approximately  $670,000$  objects over  $4780 \text{ deg}^2$  have been targeted for follow-up spectroscopy as part of SDSS are included in DR4; most spectroscopic targets are brighter than  $r = 17.77$  (Strauss et al. 2002). Automated software performs all the necessary data reduction, including the assignment of redshifts.

The Two Micron All Sky Survey (2MASS; Jarrett et al. 2000, 2003) is an all-sky map in the  $J, H,$  and  $K_s$  bands. We make use of the Extended Source Catalog, which is complete to  $K_s \sim 13.5$ . The 2MASS and SDSS catalogs are matched as described in Blanton et al. (2005), and are available in the hybrid NYU Value Added Galaxy Catalog (VAGC; Blanton et al. 2005).

In addition we use the publicly available package `kcorrect v4.1.4` (Blanton et al. 2003; Blanton & Roweis 2007) to derive restframe  $ugrizJHK$  Petrosian magnitudes for all SDSS galaxies that have a matched 2MASS counterpart. All galaxies are  $K$ -corrected to  $z = 0.0$ . The `kcorrect` package also estimates stellar masses by fitting the broad-band colors to a grid of templates based on the Bruzual & Charlot (2003) SPS code; see Blanton & Roweis (2007) for details. In §5 we will compare to these mass estimates. In the present work we are interested in deriving physical parameters for a small but representative sample of galaxies, and so we are not concerned with issues such as survey completeness or the construction of volume limited samples.

Four samples from the SDSS-2MASS matched catalog are defined in order to explore trends with luminosity and color. All galaxies are chosen to have  $0.10 < z < 0.12$  in order to minimize any possible evolutionary effects within the sample. The samples are defined according to the luminosity and color cuts defined in Table 2.

#### 4.2. Data at $z \sim 2$

In addition to data at  $z \sim 0$ , we also analyze four spectroscopically-confirmed galaxies at  $z \sim 2$  reported by Daddi et al. (2005). These galaxies lie in the *Hubble Ultra Deep Field* and have an elliptical morphology. Spectral features and broad-band colors indicate that the light from these galaxies is dominated by A- or F-type stars, and are hence not currently star-forming (Daddi et al. 2005; Maraston et al. 2006). These galaxies are interesting to study in detail because they constitute the data used by Maraston et al. (2006) to demonstrate the large systematic differences between predictions from the SPS models of Maraston (2005) and Bruzual & Charlot (2003). According to Maraston et al. (2006), these galaxies are very massive — typical stellar masses are  $\sim 10^{11} M_\odot$ .

A wide array of broad-band photometry is available for these galaxies including  $VRJK$ , *Spitzer IRAC* imaging in the  $3.6\mu\text{m}, 4.5\mu\text{m}, 5.8\mu\text{m},$  and  $8.0\mu\text{m}$  filters, and *Hubble Space Telescope* imaging in the F435, F606, F775, F895, F110, and F160W filters. Daddi et al. (2005) originally presented results for seven galaxies. We use only those galaxies that are detected in all filters and with  $z > 1.7$ , leaving us with a sample of four. Finally, we do not use the  $8.0\mu\text{m}$  filter because our

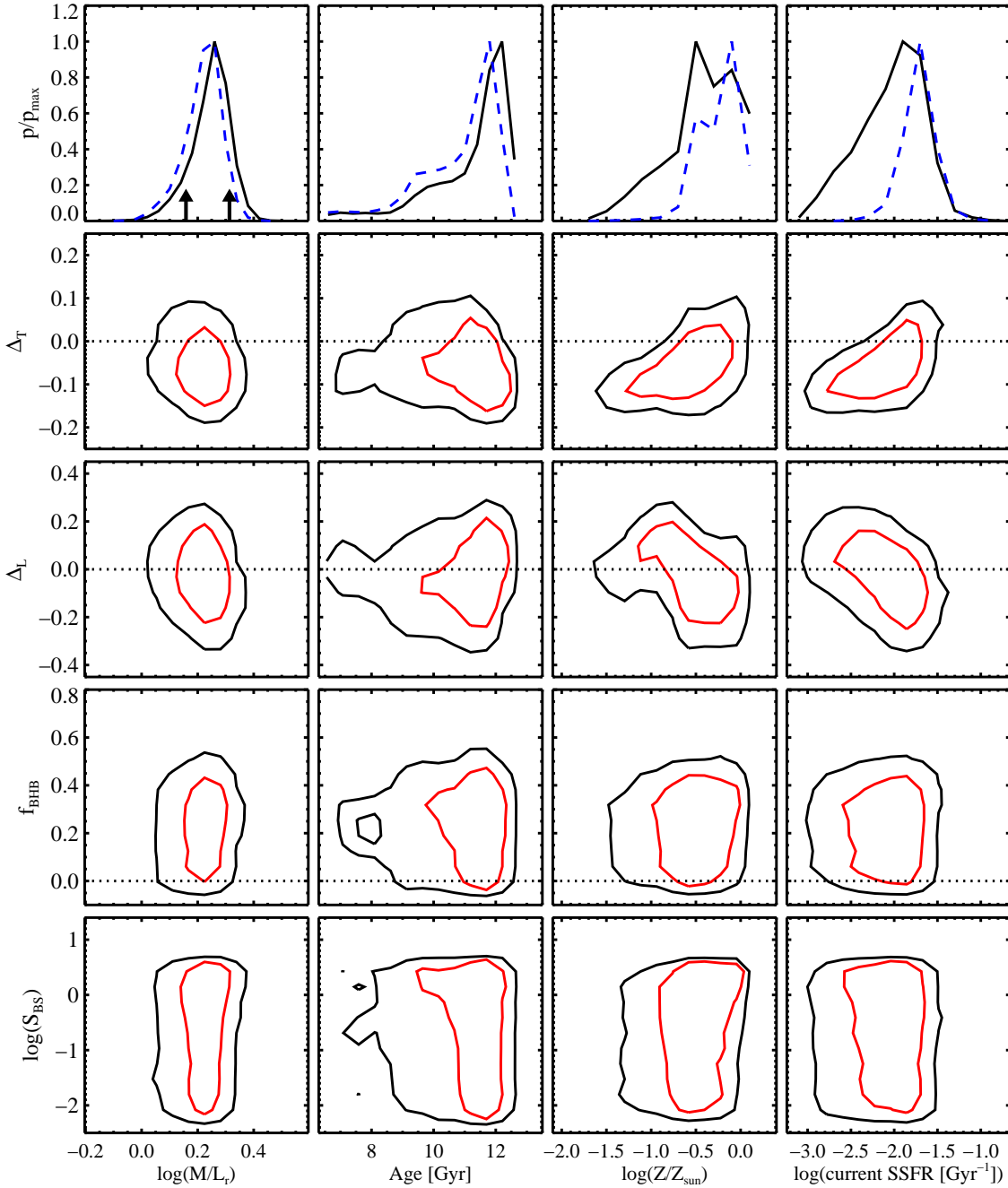


FIG. 11.— Results from fitting our SPS model to the broad-band photometry of an  $\sim L^*$  blue galaxy at  $z \sim 0$ . *Top Row*: Marginalized probability distributions for physical properties including  $M/L$ , mass-weighted age, metallicity, and current specific SFR. Results are included both for our default model with no marginalization over uncertain aspects of stellar evolution (*dashed lines*) and a model that explicitly marginalizes over such uncertain aspects (*solid lines*). The arrows in the left-most panel indicate the best fit  $M/L$  for this galaxy as determined by different authors (see the text for details). *Bottom Rows*: Likelihood contours at 68% CL (*red lines*) and 95% CL (*black lines*) highlighting the dependence of the four physical properties on four parameters governing uncertain aspects of stellar evolution (see Table 1 for details). In most cases the upper and lower bounds on the parameters along the y-axis are governed by the choice of priors. The dotted lines highlight the values of the parameters assumed in the default model. The default value for the quantity along the bottom row,  $\log(S_{BS})$ , is  $S_{BS} = 0$  and hence is not visible in the figure.

stellar libraries do not extend that far into the infrared.

#### 4.3. Fitting procedure

The SPS model outlined in §2 and 3 contains 10 free parameters, summarized in Table 1 (we do not attempt to marginalize over the IMF parameter  $m_c$ ). Recall that each point in

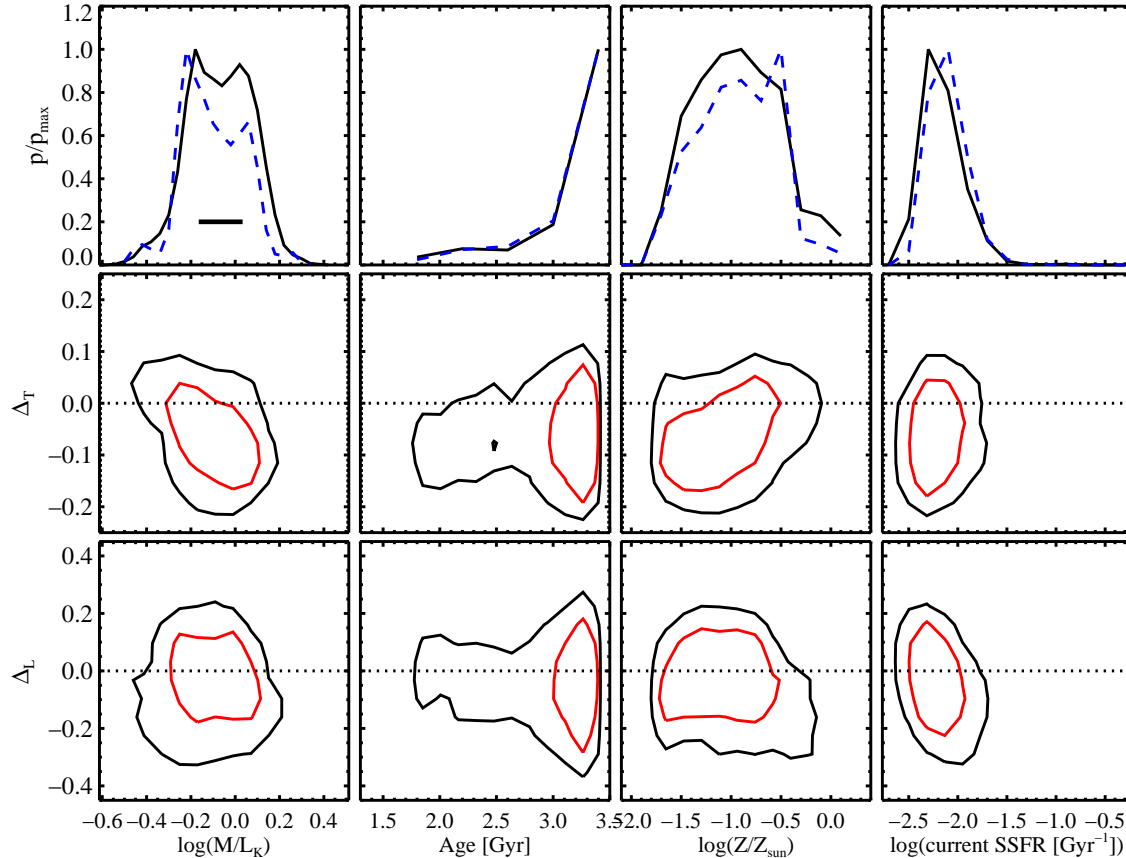


FIG. 12.— Same as Figure 11, except now for a bright red galaxy at  $z \sim 2$ . The horizontal line in the upper-left panel indicates the 95% CL limit on  $\log(M/L_K)$  for this galaxy as reported by Maraston et al. (2006, this is galaxy 3650 according to their Table 3), whose full width is 0.2 dex. According to our SPS model, the 95% CL limit on  $\log(M/L_K)$  for this galaxy is 0.6 dex. The age of the Universe at the redshift of this object is 3.6 Gyr for our adopted cosmology. The likelihood contours involving the parameters  $f_{BHB}$  and  $S_{BS}$  are not included here because those aspects of stellar evolution are assumed to turn on in our model for ages  $> 5$  Gyr, which is older than the age of the Universe at the redshift of this galaxy.

this parameter space is associated with a spectrum of a composite stellar population that can be transformed into a set of broad-band colors. Each set of parameters also specifies a time-dependent mass-to-light ratio,  $M/L$ , in a variety of filters. Our goal now is to explore the likelihood surface in this 11 dimensional space for each of a large number of observed galaxies. In particular, we are interested in the likelihood of  $M/L$  for a given galaxy.

Exploration of such a large parameter space is most efficiently accomplished with a Monte Carlo Markov Chain (MCMC) algorithm. In the MCMC algorithm, a step is taken in parameter space and this step is accepted if the new location has a lower  $\chi^2$  compared to the previous location, and is accepted with probability  $e^{-\Delta\chi^2/2}$  if the  $\chi^2$  is higher than the previous location. Each step in the chain is recorded. Since the acceptance of a step is dependent on  $\chi^2$ , most of the time will be spent in regions of high likelihood. After a sufficient number of steps the likelihood surface produced by the chain will converge to the true underlying likelihood. Convergence is defined according to the prescription described in Dunkley et al. (2005).

A set of priors are specified in order to avoid un-physical regions of parameter space. The TP-AGB parameters,  $\Delta_L$  and  $\Delta_T$ , have Gaussian priors with zero mean and standard de-

viations of 0.15 and 0.10 respectively. Uniform priors are adopted for all other parameters over the ranges shown in Table 1. All quantities are logarithmically incremented except for the TP-AGB parameters, which are already defined in the logarithm, and  $T_{start}$ , which is incremented in the quantity  $\log(T_{univ} - T_{start})$ , where  $T_{univ}$  is the age of the Universe at the redshift of the galaxy. The ranges for the parameters that incorporate uncertainties in stellar evolution are motivated in §3.

## 5. RESULTS: FROM LIGHT TO PHYSICAL PROPERTIES

This section contains the results from fitting our SPS model to data both at  $z \sim 0$  and  $z \sim 2$ . In this section we perform fits to the data both for a ‘default’ model where the isochrones are not modified ( $\Delta_T = 0$ ,  $\Delta_L = 0$ ,  $f_{BHB} = 0$ , and  $S_{BS} = 0$ ) and for a model that allows flexibility in uncertain phases of stellar evolution, as discussed in detail in §3. The goal here is to investigate to what extent, if any, the uncertainties in stellar evolution propagate into the central values and uncertainties of physical properties such as stellar masses, mass-weighted ages, and star formation rates of galaxies.

Here our aim is to highlight with representative examples the main trends and results from fitting our SPS model to data. To this end we have chosen to focus on four classes of galax-

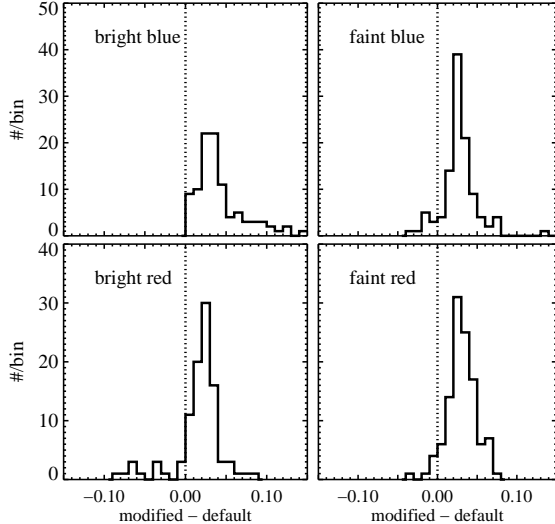


FIG. 13.— Difference between the modified and default SPS models for the best-fit  $\log(M/L_r)$  for galaxies of different types at  $z \sim 0$ . The modified models, which incorporate uncertain aspects of stellar evolution into the SPS formalism, favor slightly heavier galaxies, though the difference is well within the typical uncertainties ( $\sim 0.2$ – $0.4$  dex). Note that there is no systematic trend between the four different galaxy types defined in Table 2.

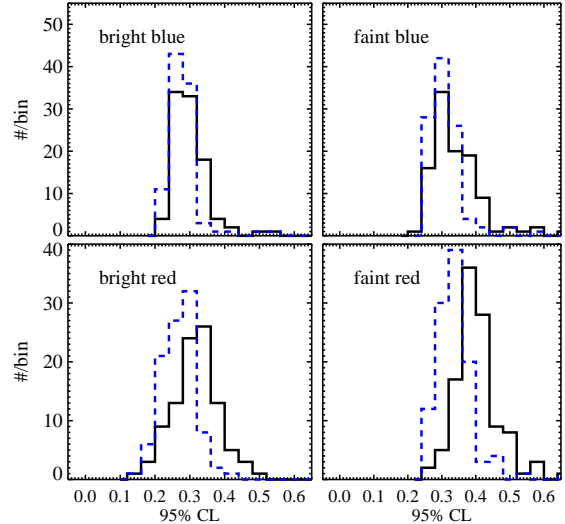


FIG. 14.— 95% confidence limits on  $\log(M/L_r)$  for samples of galaxies at  $z \sim 0$  defined according to their  $r$ -band luminosities and  $g-r$  colors. For each galaxy, the 95% CL is computed both for an SPS model that incorporates uncertainties in stellar evolution (*solid lines*) and a model that does not include such uncertainties (*dashed lines*).

ies at  $z \sim 0$ : bright red, faint red, bright blue, and faint blue galaxies as defined in Table 2.

In addition, we discuss results from fitting our model to passively-evolving luminous galaxies at  $z \sim 2$ . As mentioned above, we have chosen this last set of galaxies because such galaxies were studied by Maraston et al. (2006) who found that the different treatments of the TP-AGB phase in the SPS codes of Bruzual & Charlot (2003) and Maraston (2005) lead to large, systematic differences in stellar masses and ages of galaxies. The Maraston (2005) models yielded galaxies that were both younger and less massive than the models of Bruzual & Charlot (2003). Since TP-AGB stars dominate the stellar light at ages of  $\sim 2$  Gyr, we expect these passive galaxies at  $z \sim 2$ , which are dominated by stars at this age, to be the galaxy type most sensitive to the uncertainties associated with the TP-AGB phase. They can thus be considered a ‘worst-case scenario’ for the propagation of uncertainties in stellar evolution into parameters such as stellar mass and age.

Future work will focus on the consequences of the results presented in this section with a more statistically complete sample of galaxies.

### 5.1. Central values and uncertainties

Figures 11 and 12 show results from fitting our SPS model to the broad-band photometry of an  $\sim L^*$  blue galaxy at  $z \sim 0$ , and a luminous red galaxy at  $z \sim 2$ , respectively. The top row of panels show the marginalized probability distribution for the mass-to-light ratio, mean age, metallicity, and current specific star formation rate ( $SSFR \equiv SFR/M$ ). Results are shown for both a default model where the isochrones are fixed (*dashed lines*) and a model where aspects of the isochrones are parameterized and marginalized over (*solid lines*). The arrows in the first panel indicate the best-fit  $M/L_r$  from Kauffmann et al. (2003a) and Blanton & Roweis (2007).

The lower four rows highlight the dependence of these four physical parameters on four parameters that characterize un-

certain aspects of stellar evolution. These parameters are the temperature and luminosity of the TP-AGB phase ( $\Delta_T$  and  $\Delta_L$ ), the fraction of blue horizontal branch stars ( $f_{BHB}$ ), and the specific frequency of blue straggler stars ( $S_{BS}$ ). Both 68% and 95% CL contours are included. The dotted lines indicate the values of the parameters assumed in the default model. In Figure 12, plots associated with the parameters  $f_{BHB}$  and  $S_{BS}$  have been omitted because the age of the Universe at the redshift of this galaxy (3.6 Gyr) is younger than when these parameters are assumed to turn on (i.e. for stellar ages older than 5 Gyr).

The most striking result from these two figures is the lack of a strong degeneracy between any of the physical parameters (along the  $x$ -axis) and any of the parameters quantifying uncertain aspects of stellar evolution (along the  $y$ -axis). In Figure 11 there are weak degeneracies between TP-AGB parameters ( $\Delta_T$  and  $\Delta_L$ ) and  $SSFR$  and metallicity. The lack of any strong degeneracies in Figure 12 is even more surprising in light of the fact that the Maraston et al. (2006) and Bruzual & Charlot (2003) SPS models, which have different treatments of the TP-AGB phase, produce systematically different stellar masses. In other words, these two SPS models have different values for  $\Delta_T$  and  $\Delta_L$ , so one might have expected a degeneracy between  $M/L$  and either or both of these TP-AGB parameters. The reason for the lack of any strong dependence in the present work is due to the varying quality of fit for different TP-AGB parameters; this issue is discussed in detail in §5.2.

Despite a lack of strong degeneracies between parameters, the marginalized probability distributions for the physical parameters are clearly broader, in certain cases, for the modified compared to the default models. In particular, in Figure 11 the probability distributions of preferred metallicities and current specific star formation rates are substantially broader for the modified models. This indicates that our knowledge of these quantities is substantially impacted by uncertainties associ-

ated with stellar evolution calculations. Notice also that the uncertainty associated with  $M/L_K$  in Figure 12 is a factor of three larger than quoted in Maraston et al. (2006). The reason for this difference is not immediately clear, but may be due to the fact that we allow for more flexibility in all aspects of the SPS modeling including the SFH and dust prescription.

The parameters  $f_{BHB}$  and  $S_{BS}$  are essentially unconstrained by the data (the likelihood contours span the entire range allowed by our priors). This is due to the combined facts that these parameters are only important in the blue bands (one can see in Figures 5 and 6 that they are of minor importance for bands redward of  $V$ ), and the bluest band included in the fits at  $z = 0$ , the  $u$ -band, carries a much larger uncertainty than the other bands (a factor of 2–4 times larger). Better data in the blue and ultraviolet could potentially yield tighter constraints, although the impact of dust at these wavelengths will tend to weaken any constraints.

Figure 13 plots the difference between the modified and default SPS models for the best-fit quantity  $\log(M/L_r)$  for the four sets of SDSS-2MASS galaxies described in §4. There is a systematic offset for all galaxy types of  $\sim 0.05$  dex in the sense that the modified models favor slightly higher stellar masses. The magnitude of this effect is small compared to the typical errors (see the following paragraph), and there appears to be no systematic trend with galaxy type. These two results indicate that the central values of  $M/L_r$  (and hence of stellar mass), are not particularly sensitive to the uncertain aspects of stellar evolution that we have incorporated into the modified models with respect to the particular default model that we have used. Of course, use of a different default model, such as the one used by Bruzual & Charlot (2003), would undoubtedly lead to larger differences.

In Figure 14 we show the estimated 95% confidence limits on  $\log(M/L_r)$  for four types of galaxies at  $z \sim 0$ . Uncertainties are estimated using both the modified (*solid lines*) and default (*dashed lines*) SPS models. The typical uncertainties for blue galaxies is  $\sim 0.3$  dex and is similar for both the modified and default models. In contrast, the typical uncertainties for the red galaxies are larger by  $\sim 0.05$  dex when using the modified SPS model compared to the default model. Moreover, the uncertainties range from  $\sim 0.2$  to  $> 0.4$  dex, with typical values of  $\gtrsim 0.3$  dex for the modified models.

This result is surprising at first glance since red galaxies are generally considered to have simpler star formation histories when compared to blue galaxies. The larger errors associated with red galaxies is driven by the fact that the best SPS model fits are poorer, as determined by the minimum of  $\chi^2$ , for the red compared to blue galaxies. This fact is likely related to the longstanding problem of SPS models predicting colors redder than observations by as much as  $\sim 0.1$  magnitudes (Eisenstein et al. 2001; Wake et al. 2006). It is intriguing that even with the increased flexibility of our SPS model we are unable to obtain adequate fits to the red galaxy data (as compared to the blue galaxies). The resolution to this problem may thus lie with other aspects of SPS modeling that we have not explicitly investigated (see §6.4 for a discussion of other uncertain aspects of SPS modeling not explored herein). Very recently, Maraston et al. (2009) has shown that the use of empirical stellar spectra (as opposed to empirically-calibrated theoretical spectra) results in a much better fit to the SDSS LRG colors. This is an intriguing result that clearly requires further attention.

At redshift  $z \sim 2$ , all four luminous red galaxies studied

herein carry similar stellar mass uncertainties of  $\approx 0.6$  dex (95% CL).

## 5.2. The importance of marginalizing over uncertain phases of stellar evolution

In the previous section we found that the central values and uncertainties in the physical properties of galaxies such as star formation rates, stellar masses, ages, and metallicities, are not strongly effected when incorporating uncertainties in stellar evolution such as blue straggler stars, horizontal branch morphology, and TP-AGB temperature and luminosity. At first glance these conclusions are surprising because of recent work that has shown that different treatments of the TP-AGB phase lead to systematically different estimates for the masses of galaxies (Maraston et al. 2006). In this section we explore this apparent tension in detail.

In Figures 15 and 16 we plot the best-fit  $M/L$  for a sample of galaxies at  $z \sim 2$  and at  $z \sim 0$  as a function of the TP-AGB luminosity offset  $\Delta_L$  and  $\Delta_T$ , respectively. Here we are not marginalizing over these parameters but are instead running SPS models where we have fixed these parameters to specific values. Each SPS model will thus return a best-fit  $M/L$  and a corresponding minimum in  $\chi^2$ . It is apparent from the figure that  $\Delta_L$  and  $M/L$  are anti-correlated and so, to a lesser extent, are  $\Delta_T$  and  $M/L$ . This is the trend one expects because an observed amount of flux in the near-IR, where the TP-AGB stars contribute a significant fraction of their power, can be fit by either more stars at a lower luminosity or fewer stars at higher luminosity.

This trend qualitatively echos the conclusions reached by Maraston et al. (2006) who found that more luminous TP-AGB stars lead to a lower estimated stellar mass. The difference between these conclusions and the ones reached in the previous section, where it was found that the TP-AGB parameters and  $M/L$  were not substantially degenerate, lies in the goodness-of-fit between model and data, plotted in the upper panels of Figures 15 and 16. It is apparent from the figures that the changes in  $\chi^2$  are in most cases not significant, and thus the data allow for a wide range in  $\Delta_L$ ,  $\Delta_T$  and  $M/L$ . We stress, however, that if one *fixes* the underconstrained TP-AGB parameters (as one implicitly does when choosing a particular version of a stellar evolution calculation) and performs SPS modeling of observational data, then one can in principle introduce systematic uncertainties as large as  $\sim 0.2$  dex into the best-fit  $M/L$  values.

In short, use of poor stellar evolution models can have systematic effects on the inferred physical properties of galaxies, such as  $M/L$ , unless parameters are included that encapsulate the uncertain aspects of stellar evolution directly into the fit between model and data.

In our approach we fit simultaneously for the physical properties of galaxies and the uncertain phases of stellar evolution. We can thus ask if the default libraries adequately describe the data (i.e. if the parameters capturing the uncertain phases are consistent with zero), or if the current models are deficient in certain regimes.

In Figure 17 we plot the best-fitting TP-AGB temperature offset from the default models,  $\Delta_T$ , against the best-fit metallicity for all galaxies studied herein. It is clear that near solar metallicity the current stellar models used herein can adequately describe the broad-band SDSS+2MASS data. This is not surprising because the TP-AGB models have been calibrated largely on stars in the solar neighborhood, where the

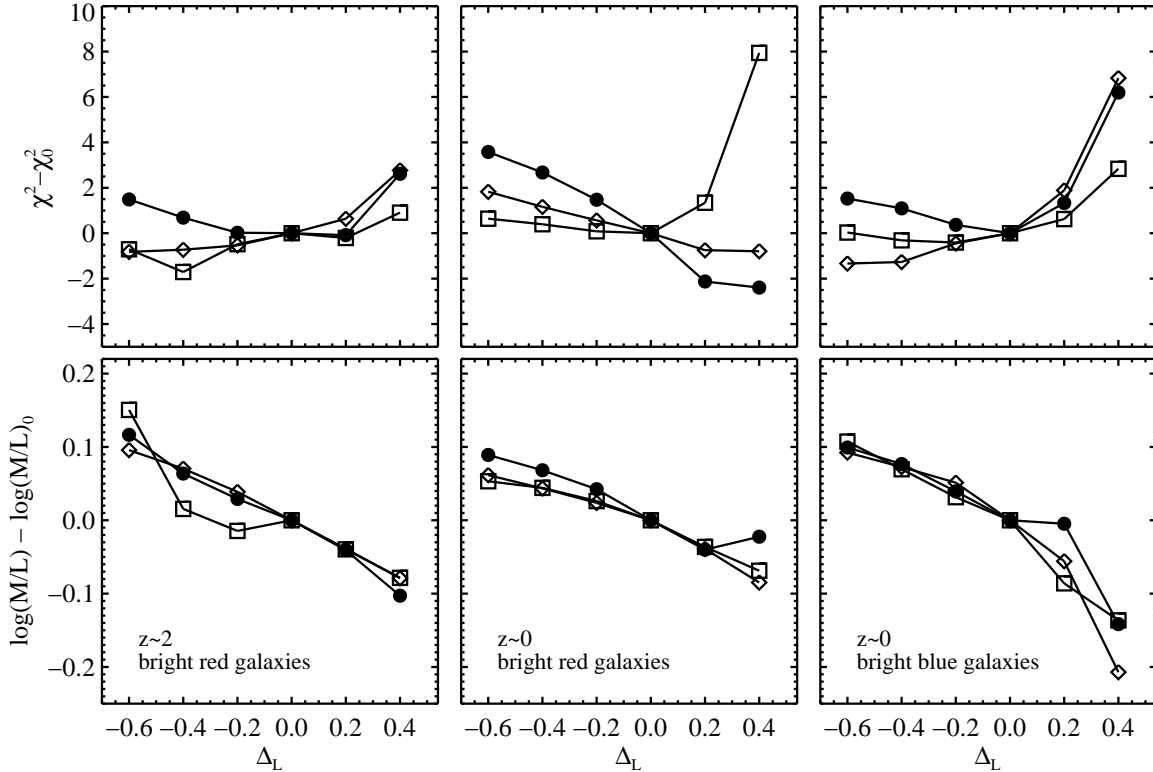


FIG. 15.— Dependence of the best-fit  $M/L$  and the minimum of  $\chi^2$  on the TP-AGB parameter  $\Delta_L$  (see Table 1 for a definition of this quantity). We plot both the best-fit  $M/L$  and the minimum of  $\chi^2$  relative to the default model where  $\Delta_L = 0$  and  $\Delta_T = 0$ . In this figure we do not marginalize over the TP-AGB parameters but instead run models for fixed values of the parameter  $\Delta_L$ , while keeping  $\Delta_T = 0$ . Trends are shown for fits to three random galaxies (*solid, diamond, and square connected symbols*) from each of the following samples: bright red galaxies at  $z \sim 2$  (*left column*), bright red galaxies at  $z \sim 0$  (*center column*), and bright blue galaxies at  $z \sim 0$  (*right column*). The trend of  $M/L$  with  $\Delta_L$  implies that use of poor TP-AGB isochrones can systematically bias the resulting  $M/L$  measurements and highlights the importance of marginalizing over the TP-AGB parameters, both at  $z \sim 2$  and  $z \sim 0$ .

mean metallicity is approximately solar (Marigo et al. 2008).

At sub-solar metallicities the temperature offset deviates substantially from zero, on average, indicating that the default models cannot adequately describe the data. The offset is in the sense that the data favor cooler TP-AGBs than the default stellar models predict. It is not altogether surprising that the default models fail in this regime because they have not been adequately tested at such low metallicities. Aside from the Milky Way, the TP-AGB isochrones have been calibrated against stars in the LMC and SMC, which have metallicities  $\sim 1/3$  and  $\sim 1/5 Z_\odot$ , respectively. Perhaps more importantly, the empirical TP-AGB spectra are largely from the solar neighborhood and both the metallicity and the metallicity dependence are not well understood (Lançon & Mouhcine 2002).

Another possible explanation is that this TP-AGB parameter is compensating for another unrelated shortcoming of the current generation of SPS models. For example, as mentioned in §2.3, the current stellar spectra libraries cannot simultaneously fit both the observed globular cluster data and the temperature-color relations of individual stars. It is beyond the scope of the present work to investigate this issue further.

These results suggest that current models are still inadequate in untested regimes, and should thus be treated with caution where extrapolations are required. We find no other strong dependence between physical parameters such

as metallicity, star formation rate, mass, or age on uncertain phases of stellar evolution.

## 6. DISCUSSION

### 6.1. The importance of accurate uncertainties

The importance of accurate and robust estimates for not only the central values of various physical properties of galaxies but also their associated uncertainties cannot be underestimated. We highlight here several areas where accurate uncertainties play an important, if often neglected role.

With the advent of large galaxy surveys and publically-available SPS codes, the estimation of stellar mass functions has become routine in both the local and distant Universe (see e.g. Cole et al. 2001; Bell et al. 2003; Fontana et al. 2004; Drory et al. 2004; Bundy et al. 2005; Borch et al. 2006). Since the mass function declines exponentially at the massive end, any uncertainty in the masses of individual galaxies can lead to a substantial misestimation of the underlying mass function. Cattaneo et al. (2008) provide illustrative examples of the extent to which uncertainties can broaden an intrinsically steep mass function. This important effect is rarely taken into account when either trying to estimate the underlying mass function or when trying to compare to models of galaxy formation. With accurate and reliable uncertainties, one can begin to deconvolve the true mass function from the broadening effects of uncertainties. This task is critical if one



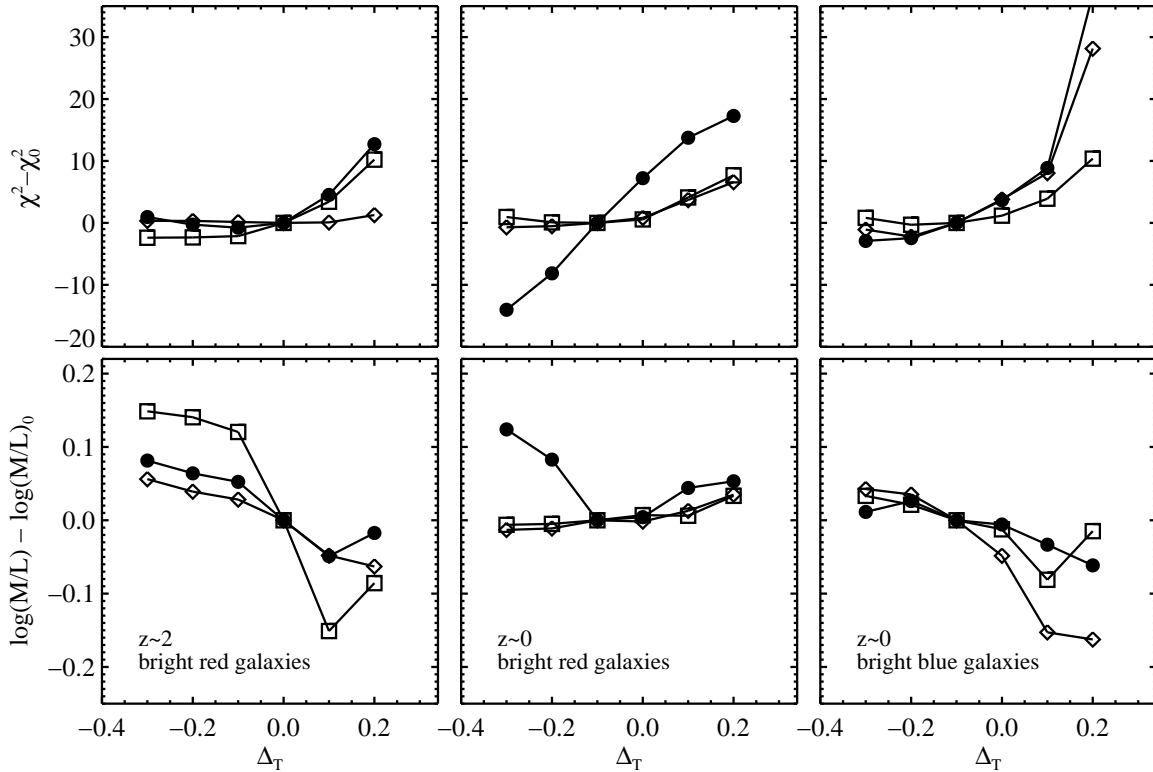


FIG. 16.— Same as Figure 15 except now plotting the best-fit  $M/L$  and the minimum of  $\chi^2$  as a function of the TP-AGB parameter  $\Delta_T$ , while keeping  $\Delta_L = 0$ .

is to make accurate comparisons to models of galaxy formation and evolution.

This concern does not reside solely with the mass function. There are many relations that are effected, including the relation between star formation rate and stellar mass, the star formation rate function, and the relation between stellar mass and large scale clustering strength. This last relation is essential for understanding the connection between galaxies and the underlying dark matter structure — an accurate accounting of the uncertainties is thus essential.

### 6.2. Why the IMF matters

As discussed in §3.4, it is extremely difficult to constrain the slope of the IMF in the solar neighborhood, let alone in external galaxies. This is unfortunate given the immense importance of the IMF in many areas of astrophysics.

For example, the IMF is not often considered a source of uncertainty when attempting to constrain the evolution of the luminosity function of galaxies through time (though see Cool et al. 2008, who discuss this source of uncertainty). In recent years it has become common to construct the luminosity function for passively evolving (i.e. red) galaxies at multiple epochs in order to understand how these galaxies grow with time. Recently, several authors have found evidence for very little intrinsic evolution in the bright end of the luminosity function of passive galaxies, suggesting that massive galaxies have evolved little since  $z \sim 1$  (e.g. Wake et al. 2006; Brown et al. 2007; Cool et al. 2008).

Passive galaxies are considered relatively easy to study be-

cause, in the absence of any appreciable star formation, the time-dependence of the luminosity of such systems is determined simply by stellar evolution and the IMF. Authors take expected luminosity evolution between two epochs for fiducial stellar evolution models and an IMF and compare to the evolution in the luminosity functions between the same two epochs in order to infer the underlying (intrinsic) change in the population with time.

We found in §3.4 however, that the uncertainty in the slope of the IMF in the solar neighborhood translates into an uncertainty in the amount of passive luminosity evolution of  $\sim 0.4$  magnitudes per unit redshift in the  $K$ -band. The difficulty of accounting for systematics in the observed IMF, and the unique difficulty of measuring the IMF slope near  $1M_\odot$  — precisely where it must be measured accurately for passive evolution corrections — suggest that this uncertainty in luminosity evolution could be an underestimate. Any possible evolution in the IMF, as discussed in §3.4, will only exacerbate this problem.

This uncertainty can have serious consequences for understanding the evolution of galaxies. We highlight one example here. There has been some tension in the literature between merger rates of luminous passive systems inferred from close-pair counts and from the evolution of the luminosity function. Taken at face value, constraints from the luminosity function suggest that the merger rate amongst bright, passive galaxies has been very modest since  $z = 1$  (Wake et al. 2006; Brown et al. 2007; Cool et al. 2008), in contrast to the apparently higher rates inferred from the close pair counts

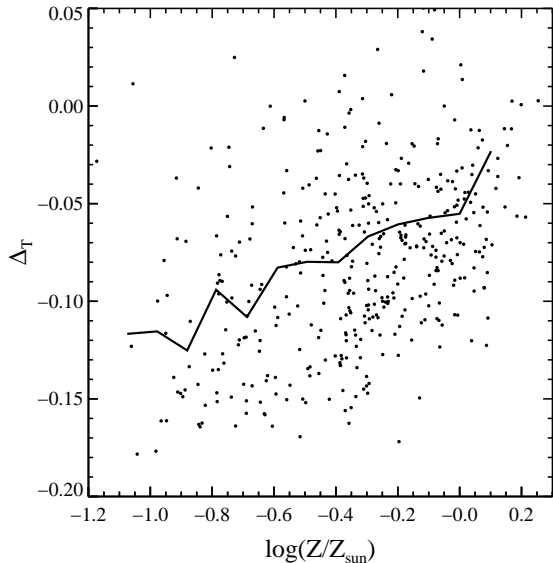


FIG. 17.— Dependence of the best-fit logarithmic temperature offset for TP-AGB stars on the best-fit metallicity for all galaxies studied herein (*symbols*). The median offset as a function of metallicity is also included (*solid line*). The temperature offset for the TP-AGB stars is defined with respect to the current stellar models, which themselves depend on metallicity. There is a clear trend that lower metallicity stars have systematically cooler TP-AGB stars than the current models predict. This is not necessarily surprising because the stellar models (including both stellar evolution and stellar atmospheres) are not calibrated at low metallicity to the precision obtained in this figure.

(van Dokkum 2005; Bell et al. 2006; Masjedi et al. 2006; Lin et al. 2008).

If the slope of the IMF were shallower than the canonical value, then from Figure 8 we conclude that luminosity evolution would be stronger than is typically assumed. If this were the case, then evolution of the luminosity function would instead require a higher merger rate than inferred with the canonical IMF slope. The slope of the IMF is thus intimately related to the merger rate as inferred from evolution of the luminosity function.

A comprehensive comparison between various merger rate indicators has yet to be undertaken, and the apparent tension in the literature between indicators may be largely interpretive. If however there is a quantitative tension, a non-canonical IMF slope may reconcile different measures.

An additional and important constraint is the evolution of the fundamental plane. As discussed in detail in van Dokkum (2008), the evolution in the fundamental plane can provide constraints on the logarithmic slope of the IMF because one can measure and compare mass evolution to luminosity evolution, so long as one is confident that the descendants of high redshift galaxies can be reliably identified at low redshift. There are additional assumptions that make it difficult in practice to set strong constraints. For example, this approach requires knowledge of the fraction of mass that is attributed to dark matter. Nonetheless, use of additional constraints, such as the fundamental plane and its evolution, can provide valuable additional constraints not only on the form of the IMF but also on uncertain aspects of stellar evolution.

### 6.3. Spectroscopy and the SDSS

We have focused on fitting our SPS model to the broad-band photometry of galaxies in the near-UV through near-IR. We now discuss the use of observed spectra in constraining SPS models.

In addition to broad-band photometry, the SDSS provides reasonable signal-to-noise, medium resolution ( $R \sim 2000$ ) spectroscopy for  $\sim 670,000$  galaxies as of DR4. These spectra provide a substantial amount of information not available in broad-band photometry. Indeed, several independent groups have made extensive use of spectroscopy to infer physical properties of SDSS galaxies (e.g. Kauffmann et al. 2003a; Panter et al. 2007).

There are several concerns related to using spectroscopy for SPS modeling that have not received extensive attention in the SPS literature. First, the robustness of the stellar spectral libraries is not known over the full luminosity, temperature, and metallicity range required. The TP-AGB spectra are clearly deficient, as described in §3.1, and will thus introduce uncertainty in the interpretation of optical and near-IR spectral features. As discussed in §2.3, there are also known systematic problems with the color-temperature relations in the stellar libraries, indicating again that the libraries probably contain unknown systematics. Furthermore, the recent results of Maraston et al. (2009) suggest that the theoretical spectral libraries are deficient in important ways.

An example of these complications was highlighted by Wild et al. (2007), who recently showed that there is a significant offset in spectral indices between the BC03 model and SDSS data. The authors attribute the mis-match to the stellar spectral libraries used in the BC03 model and caution that systematic errors in SPS models may be significantly larger than quoted statistical errors.

A second source of concern, at least for SDSS galaxies, is that the spectra are taken through fibers that only cover a fraction of the total galaxy. Averaged over the full spectroscopic sample with  $0.01 < z < 0.15$ , the spectra only captures the light from  $\approx 30\%$  of the total galaxy. For example, a galaxy may have both a bulge and a disk but the fiber would only cover the bulge and thus the spectra of this galaxy would not be representative of the total galaxy.

The standard procedure to deal with this fiber effect is to use the observed spectra in the SPS fitting and then make a correction based on the observed color(s) outside of the fiber (see e.g. Brinchmann et al. 2004). Given the unknown systematics in the spectral libraries, in conjunction with the simple correction that is typically adopted to account for light outside of the fiber, we do not believe that global physical properties of galaxies derived from spectra are more robust than information derived solely from broad-band photometry.

In fact, there is some evidence that the masses derived from spectra contain significant systematic uncertainties. Maller et al. (2009) showed that the stellar masses derived with spectroscopic information by Kauffmann et al. (2003a) are a function of the inclination of the galaxy in the sense that face-on galaxies are on average  $\approx 0.2$  dex heavier than edge-on galaxies. Of course, an intrinsic property of a galaxy such as its stellar mass should not be a function of its orientation projected on the sky. This trend thus suggests a systematic bias in the masses derived by Kauffmann et al. (2003a). The stellar masses estimated from broad-band photometry by Blanton & Roweis (2007) show a weaker dependence on inclination, and the estimates based on broad-band photometry from Bell et al. (2003) show no trend with inclination. It is not known if the trend in the spectroscopically-derived masses is

an intrinsic problem with using spectroscopic data or a systematic in the methodology of Kauffmann et al. (2003a).

#### 6.4. Additional uncertainties not explored herein

There are additional uncertainties not explored herein that may significantly impact the results of SPS modeling. In this section we briefly discuss some of the more important uncertainties.

In §2.3 we discussed several of the limitations of the current generation of stellar spectral libraries. Martins & Coelho (2007) has presented a detailed comparison between several theoretical and empirical libraries and found substantial disagreement for both blue and red colors (such as  $U-B$  and  $V-K$ , respectively). The difficulty in modeling stellar spectra is exacerbated by the fact that empirical libraries span a relatively narrow range in metallicity. Without a well-sampled empirical library it is thus difficult to understand and isolate the limitations of the models (see also Charlot et al. 1996; Charlot 1996; Yi et al. 2003).

The impact of non-solar abundance ratios has not been discussed in the present work. Observations consistently show that the  $\alpha$ -to-Fe ratio is a function of galaxy mass, with more massive galaxies being more highly  $\alpha$ -enhanced (e.g. Thomas et al. 2005). Despite this well-known observational fact, all SPS models that attempt to determine physical properties of galaxies from either their colors or spectral shapes rely on stellar spectra and evolutionary calculations with solar abundance patterns<sup>3</sup>. The effect of this omission on derived physical properties of galaxies has not been adequately quantified, but various calculations suggest that the effect can be substantial, especially for spectral signatures (see e.g. Coelho et al. 2007). The complication here is two-fold because the abundance patterns effect not only the spectra of individual stars but also the isochrones and their evolution. Fully self-consistent models of  $\alpha$ -enhanced abundance patterns are only just beginning (Coelho et al. 2007; Dotter et al. 2007; Lee et al. 2009), but early results suggest that the magnitude of this effect on colors can be as high as 0.1 magnitudes (Coelho et al. 2007).

We have not explored uncertainties in either the main sequence turn-off point or the red giant branch. Gallart et al. (2005) has presented an extensive comparison between the most popular stellar evolution models and found that slightly different treatments in the underlying physics can lead to detectable differences in derived properties such as ages and metallicities (see also Maraston 2005). For example, current stellar models predict different times for the onset of the red giant branch, owing in part to different treatments of convection in the interiors (i.e. assumptions relating to convective core overshoot and to the mixing length parameter). These differences are large enough to be detected in star clusters in the LMC (Ferraro et al. 2004), and can impact the broad-band colors of galaxies (Yi et al. 2003; Lee et al. 2007).

Another source of uncertainty that is currently not treated in SPS models is contamination of the galactic light from active galactic nuclei (AGN). Overall, the fraction of galactic light

attributed to AGN is small (e.g. Hao et al. 2005), but there are certain regimes where the contribution may be non-negligible. The problem can be particularly acute when spectroscopic information is not available to isolate AGN candidates.

## 7. SUMMARY

In this paper we have presented a novel SPS model that is capable of flexibly handling various uncertain aspects of stellar evolution including TP-AGB stars, the horizontal branch, blue stragglers, and the IMF. This model thus allows one to understand the relevance of these uncertain aspects to the derived physical properties of galaxies. In particular, one can marginalize over these uncertain aspects in order to understand the full uncertainties associated with the physical properties of galaxies including stellar masses, mean ages, metallicities, and star formation rates. We have applied this model to fit broad-band near-UV through near-IR photometry of a representative sample of galaxies at  $z \sim 0$  and  $z \sim 2$ . We have also explored the effect of the IMF on the observable properties of galaxies and have compared the stellar populations of single- to multi-metallicity stellar systems.

Significant results include the following:

1. When including the uncertainties in various stages of stellar evolution, stellar masses determined from broad-band near-UV through near-IR photometry at  $z \sim 0$  carry uncertainties of at least  $\sim 0.3$  dex at 95% CL. The masses of luminous red galaxies at  $z \sim 2$  are uncertain at the  $\sim 0.6$  dex level. The uncertainties in stellar mass are not strongly correlated with galaxy color or luminosity.
2. The TP-AGB phase in stellar evolution is clearly important for understanding the physical properties of galaxies. For example, an inadequate treatment of this uncertain phase will lead to substantial and *systematic* misestimation of stellar masses. Our SPS model suggests that either current stellar evolution calculations, model atmospheres, or both, do not adequately describe the metallicity-dependence of the TP-AGB phase. In addition, there are various degeneracies between the temperature and luminosity scale of the TP-AGB phase on the one hand, and the inferred metallicity, stellar mass, and star formation rate, on the other hand. Thus, models that do not include uncertainties in the TP-AGB phase are underestimating these derived physical properties and are potentially introducing systematic biases.
3. The uncertainties in the morphology of the horizontal branch and the frequency of blue straggler stars does not appreciably impact the SPS analysis. This is due to the fact that these aspects become increasingly important in the ultraviolet, where the data used in this analysis carry the largest uncertainties. Inclusion of more accurate ultraviolet data would probably highlight the importance of these phases in the total error budget.
4. The uncertainty in the logarithmic slope of the IMF, as determined for the solar neighborhood, implies an uncertainty in the luminosity-evolution of a passively evolving system of  $\sim 0.4$  magnitudes per unit redshift in the  $K$ -band. This is a substantial source of uncertainty that is rarely accounted for in discussions of the cosmic evolution of galaxy populations. The uncertainties associated with luminosity evolution may be even

<sup>3</sup> A considerable amount of work has gone into re-calibrating the basic outputs of solar-scaled SPS models (the SSPs) so that they may be applied more generally to variable abundance ratios. Such efforts attempt to use a variety of absorption line strengths as a diagnostic to determine the abundance patterns of individual galaxies. This method is calibrated on the abundance patterns of globular clusters for which detailed abundance patterns can be measured on a star-by-star basis. For further information see e.g. Worthey (1994); Thomas et al. (2003).

more severe both because the logarithmic slope of the IMF has not been directly measured in any external galaxy and a redshift-dependent IMF cannot be ruled out by current data.

5. The broad-band evolution of a multi-metallicity population of stars is essentially equivalent to a single-metallicity population of stars whose metallicity is the mean of the multi-metallicity population, for bands redward of  $V$ . This statement holds when one treats the morphology of the horizontal branch separately, as we have done herein. As one considers bands bluer than  $V$ , systematic differences arise between single- and multi-metallicity populations that may cause systematic biases in quantities such as galaxy ages, star formation rates, and metallicities.

In this work we have focused our attention on a limited number of broad-band filters. If significant progress is made in understanding the uncertainties in existing spectral libraries, it is possible that spectroscopy may provide much stronger constraints on the quantities of interest. In addition to spectroscopy, we leave open the possibility that carefully chosen broad- and narrow-band filters may provide stronger constraints than the filters explored herein.

For many of the uncertainties considered herein, we have adopted prior ranges that are at the extremes of, or larger than, that suggested by observational results. This is particularly the case for the range of metallicity distribution functions, horizontal branch morphology, and blue straggler specific frequency. We have demonstrated that broad-band optical through near-IR photometry is not sensitive to these uncertainties with our adopted priors, and therefore even a pessimistic assessment of our knowledge of these aspects has little effect on the derived properties of galaxies. The uncertainties listed above are more important in the ultraviolet, and we therefore expect the assumed uncertainties and priors to play a more significant role in the interpretation of restframe ultra-

violet data. Exploration of these issues will be the subject of future work.

We thank the stars for shining bright, and Tom Brown for providing his globular cluster data. This work has benefited substantially from conversations with others. We thank Raul Jimenez, Claudia Maraston, Jerry Ostriker and Pieter van Dokkum for their opinions and insights, and the referee for a careful report. This project began at the Aspen Center for Physics (partially funded by NSF-0602228) in the summer of 2007. We thank the Center for their hospitality.

Funding for the Sloan Digital Sky Survey (SDSS) has been provided by the Alfred P. Sloan Foundation, the Participating Institutions, the National Aeronautics and Space Administration, the National Science Foundation, the U.S. Department of Energy, the Japanese Monbukagakusho, and the Max Planck Society. The SDSS Web site is <http://www.sdss.org/>.

The SDSS is managed by the Astrophysical Research Consortium (ARC) for the Participating Institutions. The Participating Institutions are The University of Chicago, Fermilab, the Institute for Advanced Study, the Japan Participation Group, The Johns Hopkins University, Los Alamos National Laboratory, the Max-Planck-Institute for Astronomy (MPIA), the Max-Planck-Institute for Astrophysics (MPA), New Mexico State University, University of Pittsburgh, Princeton University, the United States Naval Observatory, and the University of Washington.

This publication makes use of data products from the Two Micron All Sky Survey, which is a joint project of the University of Massachusetts and the Infrared Processing and Analysis Center/California Institute of Technology, funded by the National Aeronautics and Space Administration and the National Science Foundation.

This work made extensive use of the NASA Astrophysics Data System and of the `astro-ph` preprint archive at [arxiv.org](http://arxiv.org).

## REFERENCES

- Abazajian, K. et al. 2004, *AJ*, 128, 502  
 Adelman-McCarthy, J. K. et al. 2006, *ApJS*, 162, 38  
 Atlee, D. W., Assef, R. J., & Kochanek, C. S. 2009, *ApJ*, 694, 1539  
 Bailyn, C. D. 1995, *ARA&A*, 33, 133  
 Baraffe, I., Chabrier, G., Allard, F., & Hauschildt, P. H. 1998, *A&A*, 337, 403  
 Bell, E. F., McIntosh, D. H., Katz, N., & Weinberg, M. D. 2003, *ApJS*, 149, 289  
 Bell, E. F., Phleps, S., Somerville, R. S., Wolf, C., Borch, A., & Meisenheimer, K. 2006, *ApJ*, 652, 270  
 Bertelli, G., Bressan, A., Chiosi, C., Fagotto, F., & Nasi, E. 1994, *A&AS*, 106, 275  
 Bessell, M. S., Brett, J. M., Scholz, M., & Wood, P. R. 1991, *A&AS*, 89, 335  
 Blanton, M. R. & Roweis, S. 2007, *AJ*, 133, 734  
 Blanton, M. R. et al. 2003, *AJ*, 125, 2348  
 —. 2005, *AJ*, 129, 2562  
 Blitz, L. & Shu, F. H. 1980, *ApJ*, 238, 148  
 Borch, A. et al. 2006, *A&A*, 453, 869  
 Brinchmann, J., Charlot, S., White, S. D. M., Tremonti, C., Kauffmann, G., Heckman, T., & Brinkmann, J. 2004, *MNRAS*, 351, 1151  
 Brown, M. J. I., Dey, A., Jannuzi, B. T., Brand, K., Benson, A. J., Brodwin, M., Croton, D. J., & Eisenhardt, P. R. 2007, *ApJ*, 654, 858  
 Brown, T. M., Bowers, C. W., Kimble, R. A., Sweigart, A. V., & Ferguson, H. C. 2000, *ApJ*, 532, 308  
 Brown, T. M. et al. 2005, *AJ*, 130, 1693  
 Bruzual, A. G. 2007, in *IAU Symposium*, Vol. 241, IAU Symposium, ed. A. Vazdekis & R. F. Peletier, 125–132  
 Bruzual, G. 1983, *ApJ*, 273, 105  
 Bruzual, G. & Charlot, S. 1993, *ApJ*, 405, 538  
 —. 2003, *MNRAS*, 344, 1000  
 Bundy, K., Ellis, R. S., & Conselice, C. J. 2005, *ApJ*, 625, 621  
 Bundy, K. et al. 2006, *ApJ*, 651, 120  
 Cassisi, S., Castellani, V., Ciarcelluni, P., Piotto, G., & Zoccali, M. 2000, *MNRAS*, 315, 679  
 Catalán, S., Isern, J., García-Berro, E., & Ribas, I. 2008, *MNRAS*, 387, 1693  
 Cattaneo, A., Dekel, A., Faber, S. M., & Guiderdoni, B. 2008, *MNRAS*, 389, 567  
 Chabrier, G. 2003, *PASP*, 115, 763  
 Charlot, S. 1996, in *Astronomical Society of the Pacific Conference Series*, Vol. 98, *From Stars to Galaxies: the Impact of Stellar Physics on Galaxy Evolution*, 275  
 Charlot, S. & Fall, S. M. 2000, *ApJ*, 539, 718  
 Charlot, S., Worthey, G., & Bressan, A. 1996, *ApJ*, 457, 625  
 Cid Fernandes, R., Mateus, A., Sodré, L., Stasińska, G., & Gomes, J. M. 2005, *MNRAS*, 358, 363  
 Cioni, M.-R. L., Girardi, L., Marigo, P., & Habing, H. J. 2006, *A&A*, 448, 77  
 Coelho, P., Bruzual, G., Charlot, S., Weiss, A., Barbuy, B., & Ferguson, J. W. 2007, *MNRAS*, 382, 498  
 Cole, S. et al. 2001, *MNRAS*, 326, 255  
 Cool, R. J. et al. 2008, *ApJ*, 682, 919  
 Daddi, E. et al. 2005, *ApJ*, 626, 680  
 —. 2007, *ApJ*, 670, 156  
 Davé, R. 2008, *MNRAS*, 385, 147  
 Davies, M. B., Piotto, G., & de Angeli, F. 2004, *MNRAS*, 349, 129  
 Dorman, B., O’Connell, R. W., & Rood, R. T. 1995, *ApJ*, 442, 105

- Dotter, A., Chaboyer, B., Ferguson, J. W., Lee, H.-c., Worthey, G., Jevremović, D., & Baron, E. 2007, *ApJ*, 666, 403
- Drory, N., Bender, R., Feulner, G., Hopp, U., Maraston, C., Snigula, J., & Hill, G. J. 2004, *ApJ*, 608, 742
- Dunkley, J., Bucher, M., Ferreira, P. G., Moodley, K., & Skordis, C. 2005, *MNRAS*, 356, 925
- Duquennoy, A. & Mayor, M. 1991, *A&A*, 248, 485
- Eisenstein, D. J. et al. 2001, *AJ*, 122, 2267
- Elmegreen, B. G. 2009, in *The Evolving ISM in the Milky Way and Nearby Galaxies*
- Ferraro, F. R., Origlia, L., Testa, V., & Maraston, C. 2004, *ApJ*, 608, 772
- Fioc, M. & Rocca-Volmerange, B. 1997, *A&A*, 326, 950
- Fontana, A. et al. 2004, *A&A*, 424, 23
- Gallart, C., Zoccali, M., & Aparicio, A. 2005, *ARA&A*, 43, 387
- Gallazzi, A., Charlot, S., Brinchmann, J., White, S. D. M., & Tremonti, C. A. 2005, *MNRAS*, 362, 41
- Girardi, L., Bressan, A., Bertelli, G., & Chiosi, C. 2000, *A&AS*, 141, 371
- Girardi, L., Chiosi, C., Bertelli, G., & Bressan, A. 1995, *A&A*, 298, 87
- Greggio, L. & Renzini, A. 1990, *ApJ*, 364, 35
- Hao, L. et al. 2005, *AJ*, 129, 1795
- Harris, W. E. 1996, *AJ*, 112, 1487
- Hopkins, A. M. & Beacom, J. F. 2006, *ApJ*, 651, 142
- Jarrett, T. H., Chester, T., Cutri, R., Schneider, S., Skrutskie, M., & Huchra, J. P. 2000, *AJ*, 119, 2498
- Jarrett, T. H., Chester, T., Cutri, R., Schneider, S. E., & Huchra, J. P. 2003, *AJ*, 125, 525
- Jimenez, R., Flynn, C., & Kotoneva, E. 1998, *MNRAS*, 299, 515
- Jimenez, R., MacDonald, J., Dunlop, J. S., Padoan, P., & Peacock, J. A. 2004, *MNRAS*, 349, 240
- Kalirai, J. S. et al. 2007, *ApJ*, 671, 748
- Kannappan, S. J. & Gawiser, E. 2007, *ApJ*, 657, L5
- Kauffmann, G. et al. 2003a, *MNRAS*, 341, 33
- . 2003b, *MNRAS*, 341, 54
- Kriek, M. et al. 2006, *ApJ*, 645, 44
- Kroupa, P. 2001, *MNRAS*, 322, 231
- Kyeong, J.-M., Tseng, M.-J., & Byun, Y.-I. 2003, *A&A*, 409, 479
- Lada, C. J. 2006, *ApJ*, 640, L63
- Lançon, A. & Mouhcine, M. 2002, *A&A*, 393, 167
- Lançon, A. & Wood, P. R. 2000, *A&AS*, 146, 217
- Larson, R. B. 1972, *Nature*, 236, 7
- . 1998, *MNRAS*, 301, 569
- . 2005, *MNRAS*, 359, 211
- Lee, H.-c., Gibson, B. K., Flynn, C., Kawata, D., & Beasley, M. A. 2004, *MNRAS*, 353, 113
- Lee, H.-c., Lee, Y.-W., & Gibson, B. K. 2002, *AJ*, 124, 2664
- Lee, H.-c., Worthey, G., Dotter, A., Chaboyer, B., Jevremović, D., Baron, E., Briley, M. M., Ferguson, J. W., Coelho, P., & Trager, S. C. 2009, *ApJ*, 694, 902
- Lee, H.-c., Worthey, G., Trager, S. C., & Faber, S. M. 2007, *ApJ*, 664, 215
- Lee, H.-c., Yoon, S.-J., & Lee, Y.-W. 2000, *AJ*, 120, 998
- Lee, Y.-W., Demarque, P., & Zinn, R. 1990, *ApJ*, 350, 155
- . 1994, *ApJ*, 423, 248
- Leitherer, C. & Heckman, T. M. 1995, *ApJS*, 96, 9
- Lejeune, T., Cuisinier, F., & Buser, R. 1997, *A&AS*, 125, 229
- . 1998, *A&AS*, 130, 65
- Li, Z.-M. & Han, Z.-W. 2009, *Research in Astronomy and Astrophysics*, 9, 191
- Lin, L. et al. 2008, *ApJ*, 681, 232
- Lucatello, S., Gratton, R. G., Beers, T. C., & Carretta, E. 2005, *ApJ*, 625, 833
- Maller, A. H., Berlind, A. A., Blanton, M. R., & Hogg, D. W. 2009, *ApJ*, 691, 394
- Maraston, C. 1998, *MNRAS*, 300, 872
- . 2005, *MNRAS*, 362, 799
- Maraston, C., Daddi, E., Renzini, A., Cimatti, A., Dickinson, M., Papovich, C., Pasquali, A., & Pirzkal, N. 2006, *ApJ*, 652, 85
- Maraston, C., Strömbäck, G., Thomas, D., Wake, D. A., & Nichol, R. C. 2009, *MNRAS*, 394, L107
- Maraston, C. & Thomas, D. 2000, *ApJ*, 541, 126
- Marigo, P. & Girardi, L. 2007, *A&A*, 469, 239
- Marigo, P., Girardi, L., Bressan, A., Groenewegen, M. A. T., Silva, L., & Granato, G. L. 2008, *A&A*, 482, 883
- Martins, L. P. & Coelho, P. 2007, *MNRAS*, 381, 1329
- Masjedi, M. et al. 2006, *ApJ*, 644, 54
- McCrea, W. H. 1964, *MNRAS*, 128, 147
- Ocvirk, P., Pichon, C., Lançon, A., & Thiébaud, E. 2006, *MNRAS*, 365, 46
- Pagel, B. E. J. 1997, *Nucleosynthesis and Chemical Evolution of Galaxies (Nucleosynthesis and Chemical Evolution of Galaxies, by Bernard E. J. Pagel, pp. 392. ISBN 0521550610. Cambridge, UK: Cambridge University Press, October 1997.)*
- Panter, B., Jimenez, R., Heavens, A. F., & Charlot, S. 2007, *MNRAS*, 378, 1550
- Papovich, C., Dickinson, M., & Ferguson, H. C. 2001, *ApJ*, 559, 620
- Persson, S. E., Aaronson, M., Cohen, J. G., Frogel, J. A., & Matthews, K. 1983, *ApJ*, 266, 105
- Piotto, G. et al. 2004, *ApJ*, 604, L109
- Preston, G. W. & Sneden, C. 2000, *AJ*, 120, 1014
- Rana, N. C. 1991, *ARA&A*, 29, 129
- Renzini, A. & Buzzoni, A. 1986, in *Astrophysics and Space Science Library*, Vol. 122, *Spectral Evolution of Galaxies*, ed. C. Chiosi & A. Renzini, 195–231
- Renzini, A. & Ciotti, L. 1993, *ApJ*, 416, L49
- Rich, R. M. 1990, *ApJ*, 362, 604
- Rich, R. M. et al. 1997, *ApJ*, 484, L25
- Salpeter, E. E. 1955, *ApJ*, 121, 161
- Sandage, A. R. 1953, *AJ*, 58, 61
- Sarajedini, A. et al. 2007, *AJ*, 133, 1658
- Scalo, J., Vazquez-Semadeni, E., Chappell, D., & Passot, T. 1998, *ApJ*, 504, 835
- Scalo, J. M. 1986, *Fundamentals of Cosmic Physics*, 11, 1
- Schaller, G., Schaerer, D., Meynet, G., & Maeder, A. 1992, *A&AS*, 96, 269
- Schiavon, R. P. 2007, *ApJS*, 171, 146
- Searle, L. & Sargent, W. L. W. 1972, *ApJ*, 173, 25
- Shapley, A. E., Steidel, C. C., Erb, D. K., Reddy, N. A., Adelberger, K. L., Pettini, M., Barmby, P., & Huang, J. 2005, *ApJ*, 626, 698
- Strauss, M. A. et al. 2002, *AJ*, 124, 1810
- Sweigart, A. V. 1987, *ApJS*, 65, 95
- Thomas, D., Maraston, C., & Bender, R. 2003, *MNRAS*, 339, 897
- Thomas, D., Maraston, C., Bender, R., & Mendes de Oliveira, C. 2005, *ApJ*, 621, 673
- Tinsley, B. M. 1980, *Fundamentals of Cosmic Physics*, 5, 287
- Tinsley, B. M. & Gunn, J. E. 1976, *ApJ*, 203, 52
- Trager, S. C., Worthey, G., Faber, S. M., & Dressler, A. 2005, *MNRAS*, 362, 2
- Tumlinson, J. 2007a, *ApJ*, 665, 1361
- . 2007b, *ApJ*, 664, L63
- van Dokkum, P. G. 2005, *AJ*, 130, 2647
- . 2008, *ApJ*, 674, 29
- Vazdekis, A. 1999, *ApJ*, 513, 224
- Wake, D. A. et al. 2006, *MNRAS*, 372, 537
- Westera, P., Lejeune, T., Buser, R., Cuisinier, F., & Bruzual, G. 2002, *A&A*, 381, 524
- Westera, P., Samland, M., Kautsch, S. J., Buser, R., & Ammon, K. 2007, *A&A*, 465, 417
- Wild, V., Kauffmann, G., Heckman, T., Charlot, S., Lemson, G., Brinchmann, J., Reichard, T., & Pasquali, A. 2007, *MNRAS*, 381, 543
- Wilkins, S. M., Trentham, N., & Hopkins, A. M. 2008, *MNRAS*, 385, 687
- Worthey, G. 1994, *ApJS*, 95, 107
- Worthey, G., Dorman, B., & Jones, L. A. 1996, *AJ*, 112, 948
- Worthey, G., España, A., MacArthur, L. A., & Courteau, S. 2005, *ApJ*, 631, 820
- Xin, Y. & Deng, L. 2005, *ApJ*, 619, 824
- Yi, S., Demarque, P., Kim, Y.-C., Lee, Y.-W., Ree, C. H., Lejeune, T., & Barnes, S. 2001, *ApJS*, 136, 417
- Yi, S. K. 2003, *ApJ*, 582, 202
- Yi, S. K., Kim, Y.-C., & Demarque, P. 2003, *ApJS*, 144, 259
- York, D. G. et al. 2000, *AJ*, 120, 1579
- Zoccali, M. et al. 2003, *A&A*, 399, 931